

## APPLIED PHYSICS REVIEWS

**Will we exceed 50% efficiency in photovoltaics?**Antonio Luque<sup>a)</sup>*Instituto de Energía Solar, Universidad Politécnica de Madrid, 28040 Madrid, Spain*

(Received 2 April 2011; accepted 25 May 2011; published online 8 August 2011)

Solar energy is the most abundant and reliable source of energy we have to provide for the multi-terawatt challenge we are facing. Although huge, this resource is relatively dispersed. High conversion efficiency is probably necessary for cost effectiveness. Solar cell efficiencies above 40% have been achieved with multijunction (MJ) solar cells. These achievements are here described. Possible paths for improvement are hinted at including third generation photovoltaics concepts. It is concluded that it is very likely that the target of 50% will eventually be achieved. This high efficiency requires operating under concentrated sunlight, partly because concentration helps increase the efficiency but mainly because the cost of the sophisticated cells needed can only be paid by extracting as much electric power from each cell as possible. The optical challenges associated with the concentrator optics and the tools for overcoming them, in particular non-imaging optics, are briefly discussed and the results and trends are described. It is probable that optical efficiency over 90% will be possible in the future. This would lead to a module efficiency of 45%. The manufacturing of a concentrator has to be addressed at three levels of integration: module, array, and photovoltaic (PV) subfield. The PV plant as a whole is very similar than a flat module PV plant with two-axes tracking. At the module level, the development of tools for easy manufacturing and quality control is an important topic. Furthermore, they can accommodate in different position cells with different spectral sensitivities so complementing the effort in manufacturing MJ cells. At the array level, a proper definition of the nameplate watts, since the diffuse light is not used, is under discussion. The cost of installation of arrays in the field can be very much reduced by self aligning tracking control strategies. At the subfield level, aspects such as the self shadowing of arrays causes the CPV subfields to be sparsely packed leading to a ground efficiency, in the range of 10%, that in some cases will be below that of fixed modules of much lower cell efficiency. All this taken into account, High Concentration PV (HCPV) has the opportunity to become the cheapest of the PV technologies and beat the prevalent electricity generation technologies. Of course the way will be paved with challenges, and success is not guaranteed. © 2011 American Institute of Physics. [doi:[10.1063/1.3600702](https://doi.org/10.1063/1.3600702)]

**TABLE OF CONTENTS**

I. WHY HIGH EFFICIENCY? .....	1
II. EFFICIENCY LIMITS OF SOLAR CONVERSION .....	2
III. PUSHING THE EFFICIENCY BEYOND THE SHOCKLEY-QUEISSER LIMIT .....	4
A. Multijunction Solar Cells .....	4
B. Novel Concepts for Exceeding the SQ Limit .....	8
IV. CONCENTRATOR TECHNOLOGY FOR HIGH EFFICIENCY SOLAR CELLS .....	10
A. Optics for HCPV .....	10
B. HCPV Modules .....	12
C. HCPV Arrays .....	14
D. HCPV Subfields and Fields .....	14
V. COSTS AND MARKETS .....	16

VI. STRESSES ON MATERIALS .....	17
VII. CONCLUSIONS .....	17

**I. WHY HIGH EFFICIENCY?**

The energy consumption of Mankind, with its consequential waste, will increase enormously when, in a few decades, the consumption patterns of more than  $2 \times 10^9$  inhabitants (China, India, etc.) adopt the consumption patterns of the developed world.

Useful energy is obtained massively from few sources: coal, oil, gas (all fossil fuels) and nuclear fission. Additionally, part comes from hydropower. Biomass is also an important source of energy mainly in rural areas and mostly outside commercial circuits. The latter two are renewable and based on solar energy.

When fossil fuels burn, the exothermic reactions of the C and H atoms with oxygen produce heat at high temperature, which may be used to produce electricity or mechanical

<sup>a)</sup>Electronic mail: luque@ies-def.upm.es.

power. Additionally, CO<sub>2</sub> and H<sub>2</sub>O molecules are produced. The former is a greenhouse gas that prevents a proportion of IR radiation from escaping the Earth's atmosphere, so modifying its energy balance. There is clear evidence that since the beginning of industrialization the content of CO<sub>2</sub> in the atmosphere is continuously increasing and that this is a major contributor to climatic change. H<sub>2</sub>O molecules also constitute a greenhouse gas; however their abundance is not primarily influenced by human activity but is rather determined by the mass of water present in the oceans (although global warming would imply further H<sub>2</sub>O in the atmosphere).

The availability of fossil fuels will not last forever.<sup>1</sup> In any individual oil well, production will peak at a given moment followed by a phase of exhaustion. When oil production will peak has been the subject of many studies. Some think that peaking is already occurring. Others expect the peaking to occur in few decades. Some leaders (see for instance, e.g., using Google, numerous declarations of Dr. Fatih Birol, Chief Economist of the International Energy Agency) of the oil industry have announced that this situation is already happening and in general their statements reveal real concern. Gas is in the same situation, perhaps less exploited but moving toward peaking in the coming decades. Coal might last longer, peaking within few centuries.

In the case of the nuclear energy, heat, to be converted into electricity, is produced by the fission of uranium <sup>235</sup>U, the only natural fissile material, by absorption of neutrons, into two atoms of smaller atomic mass and several neutrons. The reaction is exothermic, because the mass of the reaction products is smaller than the mass of the reactants. The mass defect is transformed into energy according to Einstein's formula. The proportion of <sup>235</sup>U in natural uranium is around 0.7%. However, the main component of it, the isotope <sup>238</sup>U, is a fertile material that can become fissile by bombardment with neutrons forming plutonium. This latter reaction occurs to some extent in most nuclear reactors today. The energy obtained by nuclear fission does not emit greenhouse gases in its burning process. In this respect it is a clean energy. However, it produces radioactive waste, whose safe disposal is an essentially unsolved issue. We can add to this, concerns on safety. It is supposed that the consequences of a major accident are frightening but its probability is negligible. The risk is therefore undetermined due to lack of experience.

The availability<sup>1</sup> of <sup>235</sup>U is also expected to peak in several decades notwithstanding unrealistic claims to the contrary that point out the enormous amount contained in sea water, with concentrations too low for exploitation. However, the fact that the much more abundant <sup>238</sup>U is fertile may lead to many solutions with different degrees of generation of new fissile material. Other fertile materials are also naturally available or can be produced in nuclear reactors. In this regard, the availability of nuclear power can last centuries, although possibly not with very large power production (due to reduced neutron flux<sup>1</sup>).

The only solution may be the use of solar energy. The power received by the Earth from the Sun is around 6000 times Mankind's present consumption.<sup>2</sup> This has to be converted into usable energy (electricity) with high efficiency. Efficiencies

below 0.02% would not permit the supply of the present needs of Mankind, not to mention its expansion. Biomass and wind energy are related, to certain extent, to this low efficiency problem because both forms of renewable energy are derived from solar energy through the natural processes of conversion.

In contrast, photovoltaics (PV) may provide the needed high efficiency. An efficiency of about 10% for a surface normal to the sun is today possible (see Sec. 3.4) with a land occupation of about twice the module area, that implies an efficiency of 5% per unit area of land occupied. Considering only collection in terrestrial lands (1/4), the fraction necessary to provide the full present (primary, not only electric) energy consumption is 1.35%. This is much less than the space required for food (13% of the terrestrial land is cultivated and 26% is pasture)<sup>3</sup> and means that there is not a real problem of space, despite the frequent claim to the contrary. Nevertheless, high efficiency is of paramount importance. As shown in Fig. 1, efficiencies above 40% are being obtained in some laboratories for concentrator solar cells.

Photovoltaics have often been considered to be ideal for distributed electricity generation. Power supplies for remote electronic equipment, essential electricity for rural areas in developing countries, electricity for isolated homes, and, perhaps, homes and buildings that inject electricity into the electric grid were the applications thought for PV. The idea of PV power plants has indeed been contemplated but, at least in Europe and Japan, as a remote and less desirable possibility. However, driven by the high feed-in tariff, large power plants proliferated in Spain in 2008 (by the end of that year, 40 of the 50 largest plants in the world were in Spain and the tendency toward large plants continues today in many countries<sup>4</sup>). In the year 2000 it was about 1% of the 288 MW installed. In 2008 it amounted to 55% of the 5600 MW installed.<sup>5</sup> This is also a natural market for the proliferation of high concentration photovoltaics (HCPV) if it is cheaper than ordinary flat panel PV. In this paper we shall try to substantiate why and how this might be the case.

## II. EFFICIENCY LIMITS OF SOLAR CONVERSION

A solar energy converter is connected to the sun that is a reservoir of photons at about 6000 K. Assuming that the converter is also connected to a cold reservoir, the Earth, at about 300 K, the naïve answer to the question implicit in the heading is that the efficiency limit for a solar converter is the Carnot efficiency, that is, 95%.

This is however incorrect, and the reason is a matter of definition. The Sun is a reservoir of energy that, unlike conventional ones, e.g., a tank of petrol, is emitting its energy continuously in the form of solar radiation. Therefore, the preferred definition of efficiency is not the ratio of useful work performed divided by the (internal) energy taken from the hot reservoir but rather divided by the flux of solar energy collected (in a given time) by the solar converter.

Let us explain the difference further: any solar converter receives energy in the form of solar radiation, produces electric power and delivers energy in the form of heat at 300 K to the ambient, just as any other thermal machine. However, in addition, the solar converter emits radiation. This must

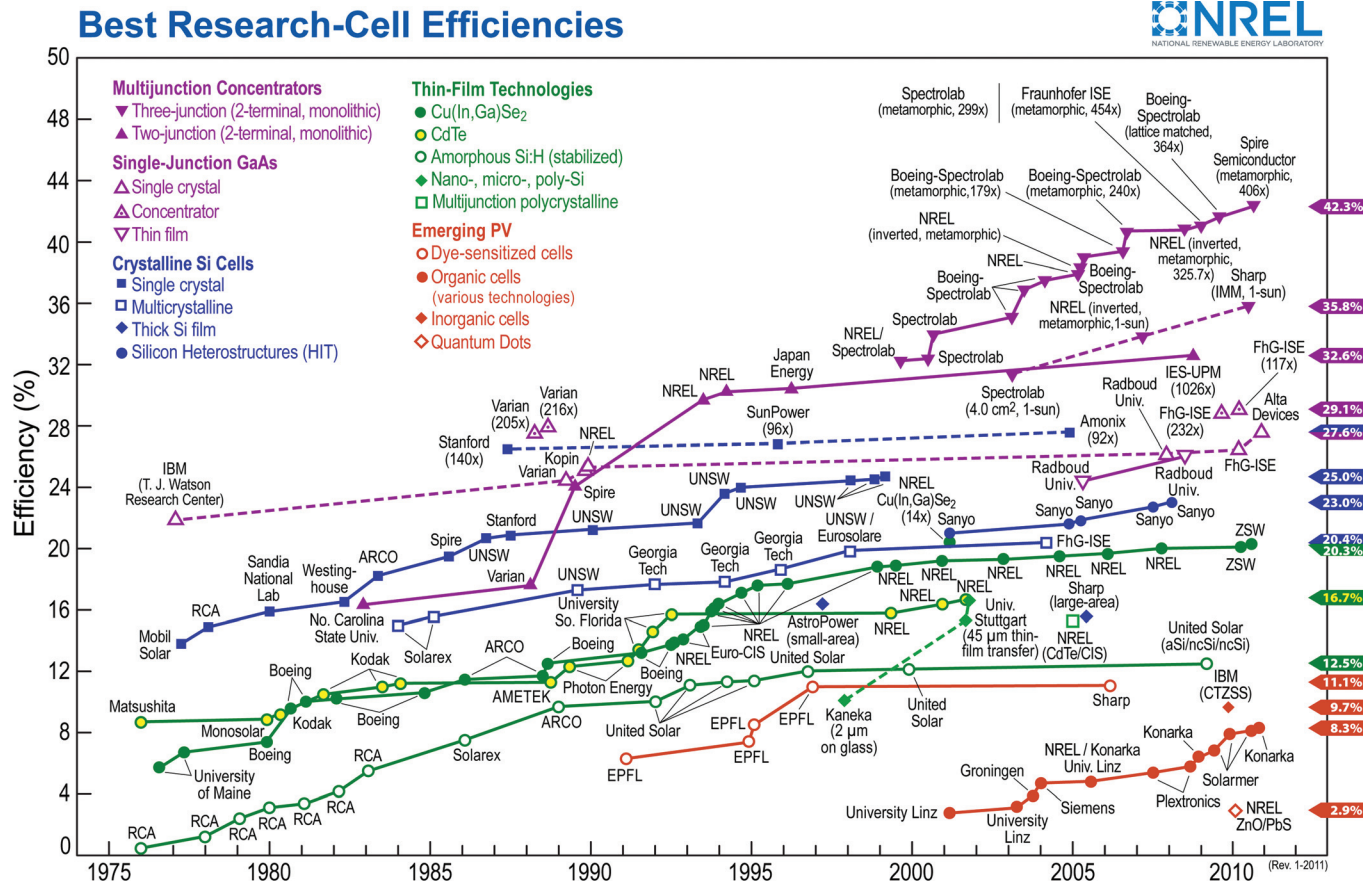


FIG. 1. (Color) Unlike most other cell types, which appear to have reached close to their maximum efficiency performance in recent years, research teams are still showing significant progress with multi-junction devices. Over the past decade, the best-performing multi-junction cells have moved from around 35% efficiency to the latest record of 42.3% achieved by Spire Semiconductor. Production line cell efficiency tends to lag the champion-cell figure by about 2 years. Courtesy of NREL (Dr. Nozik).

enter in the balance of received and emitted energy for stationary operation.

The fact that the solar converter emits radiation can be expressed by time reversal. If the rays can enter into the converter through a certain ray path, the same path may be traveled in the opposite direction by rays exiting the solar converter. This is a very fundamental principle called time micro reversibility and is fulfilled in any closed system in nature. It may be not fulfilled in some open systems, e.g., in the presence of interacting magnetic fields. We shall disregard these cases.

In the case of a solar thermal converter the emitter of radiation is the hot receiver, which obviously emits thermal radiation mostly toward the dark regions of the sky and, in a small part, toward the sun. In the case of a solar cell, the emitted radiation is luminescent radiation produced by the electron-hole excess in the cell. For emittance equal to one in the energy interval ( $\varepsilon_m$ ,  $\varepsilon_M$ ) and zero outside, the emitted radiation rate follows the modified Planck law (see e.g. Ref. 6)

$$\dot{E}(T, \mu, \varepsilon_m, \varepsilon_M, H) = \frac{2H}{h^3 c^2} \int_{\varepsilon_m}^{\varepsilon_M} \frac{\varepsilon^3 d\varepsilon}{e^{(\varepsilon-\mu)/kT} - 1} \quad (1)$$

where  $\mu$  is the photon electrochemical potential (characterizing luminescent radiation) and  $dH = n_{\text{ref}}^2 \cos \theta d\sigma dA$  is the differential of étendue<sup>7</sup> (or Lagrange invariant) of the emit-

ted bundle of rays by an element of surface  $dA$  in the solid angle element  $d\sigma$  forming an angle  $\theta$  with the surface element.  $n_{\text{ref}}$  is the index of refraction of the region where the radiation is emitted, equal to one for vacuum or air. For isotropic emission,  $H = \pi n_{\text{ref}}^2 A$ . For a cone of light of semi-angle  $\varphi$  and normal to the surface,  $H = \pi n_{\text{ref}}^2 A \sin^2 \varphi$ . The same formulae may be used for the radiation received on a surface.

In the case of an ideal solar-thermal converter  $\mu=0$ ,  $T_r$  is the temperature at which the blackbody absorber is raised by the concentrator system and  $H = \pi A$ ; the integration extends for zero to infinity giving the Stefan Boltzmann law  $\dot{E}(T_r, 0, 0, \infty, \pi A)/A = 5.67 \times 10^{-8} T^4 \text{ W m}^{-2}$ . In the case of a PV solar cell we must calculate  $\dot{E}(300, eV, E_G, \infty, \pi A)$  where  $E_G$  is the semiconductor bandgap and  $eV$  is the cell voltage that in ideal cells is the difference between the electron and hole quasi Fermi levels (QFLs).

An interesting aspect of this discussion is that we can define the type of solar receiver we are dealing with by observing the radiation emitted. If it is thermal ( $\mu=0$ ) at high temperature, the converter is solar thermal. If it is luminescent ( $\mu \neq 0$ ) at room temperature, it is photovoltaic. Hybrid options at high temperature and  $\mu \neq 0$  are conceptually possible.

With the technical definition of efficiency for solar converters, the limiting efficiency was determined by Landsberg and Tonge<sup>8</sup> and is given by

$$\eta_{\text{Landsberg}} = 1 - \frac{4}{3} \left( \frac{T_{\text{ambient}}}{T_{\text{sun}}} \right) + \frac{1}{3} \left( \frac{T_{\text{ambient}}}{T_{\text{sun}}} \right)^4. \quad (2)$$

This efficiency is achieved if the device produces zero entropy and emits its radiation to the sun (by means of an ideal concentrator, in reverse used as a collimator) as thermal radiation at ambient temperature. For the 6000/300 K Sun/ambient temperatures it gives 93.33% instead of the 95% Carnot efficiency. We do not know of any device, real or proposed, reaching the Landsberg efficiency.

The concept of étendue requires some further discussion. The étendue calculated at a given surface fully intercepting the rays in any optical system is invariant of the surface chosen.<sup>9</sup> For instance, the étendue from the Sun (apparent semi-diameter  $\varphi_{\text{sun}}$ ) on the entry aperture of an optical system is  $H = \pi A_{\text{optics}} \sin^2 \varphi_{\text{sun}}$ . If this optical system casts all the rays onto a solar cell within a semi-angle  $\varphi_{\text{optics}}$ , the étendue will be  $H = \pi A_{\text{cell}} \sin^2 \varphi_{\text{optics}}$ . The optics may be a lens, in which case  $1/2 \tan \varphi_{\text{optics}}$  is the lens  $f$ -number. Equating both expressions of the étendue we obtain  $C_g \equiv A_{\text{optics}}/A_{\text{cell}} = \sin^2 \varphi_{\text{optics}} / \sin^2 \varphi_{\text{sun}}$ . This means that for ideal optics not casting rays outside the cell this formula gives the highest possible geometrical concentration.

In 1961 William Shockley and Hans Queisser (SQ) published an elegant paper<sup>10</sup> establishing the efficiency limit of a solar cell. They considered the solar cell as a system of two levels, the valence band (VB) and the conduction band (CB) and stated that each photon with energy above the bandgap pumps one electron from the valence band to the conduction band. They assumed infinite mobility so that the CB and VB QFLs are horizontal and their difference is  $eV$  everywhere. They also assumed that selective contacts (heavily doped n and p regions) are formed so that it is possible to extract electrons and holes separately. They further assumed that all non-radiative recombination processes are suppressed and that radiative recombination is only produced by radiation that escapes by the cell surfaces. Note, not all radiative recombination is actually considered because of photon recycling, which means that the photon produced may be reabsorbed. In this way they pioneered then recent and complex models including photon recycling, albeit in an idealized way.<sup>11</sup> Thus they establish a balance equation of the photons entering and escaping the semiconductor and the electron-hole pairs produced and extracted. No mention is made to the properties of the semiconductors—excepting the bandgap—or to the need of any p-n junction.

More recently the calculations have been repeated<sup>12</sup> for the case of solar radiation impinging on the solar cell isotropically ( $H = \pi n_{\text{ref}}^2 A$ ) rather than within the natural cone of direct solar radiation ( $\varphi_{\text{sun}}$ ). We refer to this situation as full concentration. The top efficiency is 40.7% for blackbody radiation at 6000/300 K (solar/ambient) temperatures as shown in Fig. 2, together with cases for other spectra (direct and global<sup>13</sup>) and concentration levels.

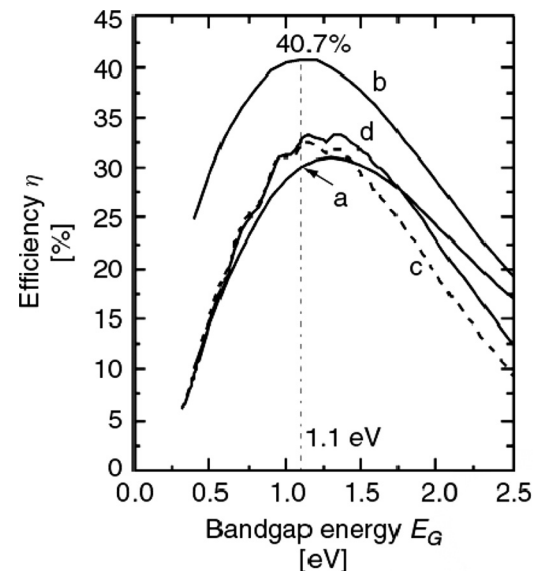


FIG. 2. SQ efficiency limit for an ideal solar cell versus bandgap energy for: (a) unconcentrated 6000 K blackbody radiation ( $1595.9 \text{ W m}^{-2}$ ); (b) fully concentrated 6000 K blackbody radiation ( $7349.0 \times 10^4 \text{ W m}^{-2}$ ); (c) unconcentrated AM1.5-Direct<sup>13</sup> ( $767.2 \text{ W m}^{-2}$ ); (d) AM1.5 Global<sup>13</sup> ( $962.5 \text{ W m}^{-2}$ ). Reprinted with permission from A. Luque and A. Martí, in Handbook of Photovoltaic Science and Engineering, 2nd edition. © 2011 Wiley.

The main reason a solar cell, even if ideal, is so far from the Landsberg efficiency is because it does not use the whole solar spectrum but only the photons with energy above the bandgap. A second reason is that entropy is generated in the cooling of the electron-hole pairs produced by high-energy photons. In fact they are delivered at the voltage of the cell, which cannot exceed the bandgap. In reality, in the ideal solar cell the open circuit voltage will not exceed  $V_{oc} = E_G(1 - T_{\text{ambient}}/T_{\text{sun}})$ .

### III. PUSHING THE EFFICIENCY BEYOND THE SHOCKLEY-QUEISSER LIMIT

An ideal photovoltaic cell covered by a narrow bandpass filter and illuminated by the monochromatic radiation traversing it would be close to producing zero entropy. It would be exactly so if the cell were in open circuit,<sup>6</sup> but then no power is extracted. This is a general rule for all reversible devices. They have to evolve very slowly between equilibrium states so that they can produce the highest work but small power.

#### A. Multijunction Solar Cells

The obvious way to manufacture a practical device based on this idea is to build a stack of solar cells of different bandgaps, usually called a multijunction (MJ) solar cell. In this way the entire solar spectrum can be used and the upper cells can act as a filter for the lower ones, each being illuminated by a narrow range of photon energies thus reducing the production of entropy. Expressed in less fundamental terms, each cell will produce current at a voltage limited by its bandgap, but this bandgap will not be much lower than the energy of the photons absorbed by the individual cell. The concept is expressed in Fig. 3.<sup>14</sup> Filters (named reflectors)

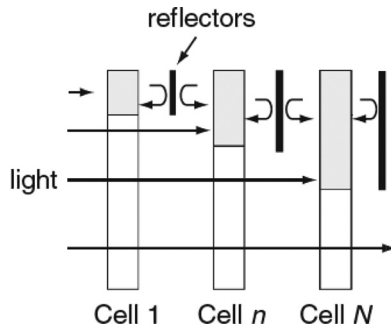


FIG. 3. Stack of solar cells ordered from left to right in decreasing bandgap ( $E_g1 > E_g2 > E_g3$ ). Reprinted with permission from A. Martí and G. L. Araújo, Sol. Energy Mater. Sol. Cells 43, 203 (1996). © 1996, Wiley.

are located between the different cells to prevent luminescent radiation produced in each cell from passing into the following cell where it would be converted with lower efficiency.<sup>12</sup> This is a refinement that as far as we know, has never been practically implemented.

For an infinite number of ideal cells, the efficiency<sup>12</sup> of this arrangement is 86.8% under full concentration for 6000/300 K sun/ambient temperature. This is below the Landsberg limit. The entropy produced is nearly zero but the luminescent radiation emitted is not thermal at room temperature.

This concept has been put into practice in many ways, including mechanical stacks of cells of different semiconductors or beam splitting filters that cast part of the spectrum on each cell.<sup>15,16</sup> The most popular concept, and the only one to discuss in this section, is the monolithic multijunction cell. This consists of solar cells of different materials along with tunnel diodes to interconnect them in series all grown on a single substrate. III–V compound semiconductors of a variety of materials can be grown epitaxially with very high quality if all the materials have a similar lattice constant. We present in Fig. 4 a plot of the bandgap versus the lattice constant of several III–V binary compounds. The bandgap and lattice constant of ternary compounds are represented by polygonal or curved lines between the binaries containing the

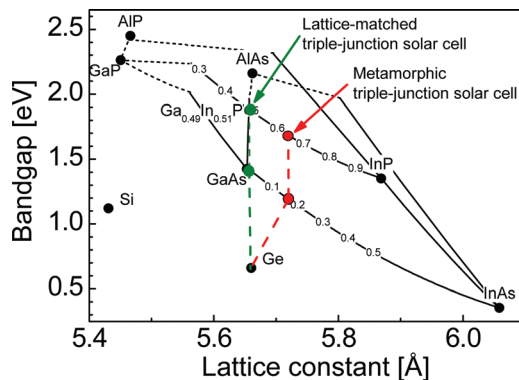


FIG. 4. (Color) Combinations of bandgap and lattice constant for various materials used in III–V solar cells. The potential substrate materials silicon (Si) and germanium (Ge) are also indicated. As an example, the bandgap combinations of the lattice-matched triple-junction solar cell on Ge as well as of a metamorphic triple-junction solar cell developed at FhG-ISE are indicated. The upper cells of the metamorphic solar cells have a lattice-mismatch of 1.2% compared to the Ge substrate. In order to achieve sufficient material quality, a buffer layer is integrated into the structure.

same elements. For instance, at a certain value of  $x$  close to 0.5, the  $\text{Ga}_x\text{In}_{1-x}\text{P}$  will have the same lattice constant as GaAs and a bandgap energy close to 1.85 eV.

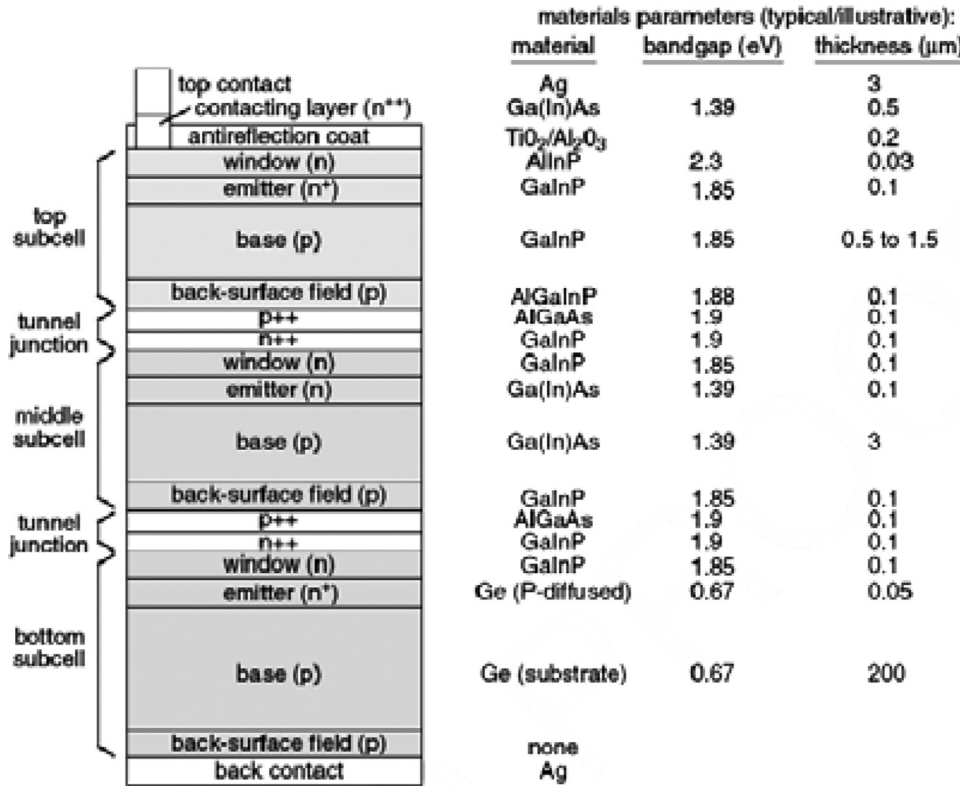
Today, stacks with up to three cells have been built on Ge substrates, whose lattice is similar to that of GaAs. A schematic is presented in Fig. 5.<sup>17</sup> The roles of the different layers are explained in the figure caption. The so called window layers are intended to prevent recombination at the surface or in the tunnel junctions. The fraction of group III elements in each layer is adjusted to obtain the desired bandgap. As stated in the figure, the data is illustrative and each manufacturer has its own recipe.

The series connection of the different cells introduces an additional constraint because the photogenerated current of the stack is the smallest of the currents generated by each cell. The best situation is when all the cells have the same photogenerated current. This restricts the efficiency of a series connected stack with respect to that of an unconstrained stack. For an infinite number of cells, the efficiency limit is the same.<sup>18</sup> However, for three cells (the configuration that is commercially available today) the efficiency limit for the unconstrained stack is 63.6% compared to 63.0% for the series connected stack, where conditions of full concentration (about 46 000 suns) and sun/ambient temperatures of 5762/298.15 K are assumed in both cases. The sun temperature considered here is that which gives the extraterrestrial spectrum and the ambient temperature is 25 °C. These are some of the commonly used standard measuring conditions. Optimal bandgaps for the series connected case are 1.75, 1.10, 0.58 eV, but optimal bandgaps at lower concentration are higher and the efficiency is lower.

Two main strategies are followed for the growth of the epitaxial cells: the lattice matched (LM) approach and the metamorphic (MM) approach. In the first case, the lattices of the different cells are as closely matched as possible. That is why a small proportion of In (1%) is added to the GaAs allowing close matching with the Ge substrate. The drawback is that this procedure does not admit optimal bandgaps for ternaries of the elements in consideration (Ga, In, P and As). This result is evident in Fig. 6,<sup>19</sup> where, for the lattice matched (LM) cell, the badgaps of the two upper cells are a bit too large. In this scheme, the upper III–V cells give too little current as compared to the Ge cell.

In the metamorphic approach the bandgaps are better adjusted at the expense of permitting the formation of threading dislocations as shown in Fig. 7. This reduces the cell quality and may balance out the advantages of better bandgap matching.

Very good results have been obtained with the present structures, the best by July 2010 (Ref. 20) being 41.6% by Spectrolab (USA) with a  $\text{Ga}_{0.5}\text{In}_{0.5}\text{P}/\text{Ga}_{0.99}\text{In}_{0.01}\text{As}/\text{Ge}$  lattice matched solar cell at 364 suns and 41.1% by Fraunhofer ISE (Germany) with a  $\text{Ga}_{0.35}\text{In}_{0.65}\text{P}/\text{Ga}_{0.83}\text{In}_{0.17}\text{As}/\text{Ge}$  metamorphic solar cell at 454 suns.<sup>17</sup> The bandgaps are 1.85, 1.39, 0.67 eV and 1.67, 1.18, 0.67 eV, respectively. In the MM2 case (that of Fraunhofer ISE) the bandgaps are near optimal. The measurements have been made at certified laboratories. However, it is worth noting that uncertainty in the measurements is given as  $\pm 2.5$  absolute percent points.<sup>21</sup>



The use of the Ge substrate is considered by some to be a serious drawback: it is expensive and not very abundant. The concept of the inverted metamorphic (IMM) growth

FIG. 5. Schematic cross-section of a monolithic two-terminal series-connected three-junction solar cell. An n-on-p configuration is illustrated. Doping indicated by  $n^{++}$ ,  $n^+$  and  $n$  (or  $p^{++}$ ,  $p^+$ ,  $p$ ) corresponds to electron (or hole) concentrations of the order of  $10^{19}$ – $10^{20}$ ,  $10^{18}$  and  $10^{17} \text{ cm}^{-3}$ , respectively. Typical materials, bandgaps, and layer thicknesses for the realization of this device structure as a GaInP/GaAs/Ge cell are indicated. Note that not all layers in an actual device (e.g., tunnel-junction cladding layers) are included in the illustration. The figure is not to scale. Reprinted with permission from D. J. Friedman, J. M. Olson, and S. Kurtz, in *Handbook of Photovoltaic Science and Engineering*, 2nd edition. © 2011, Wiley.

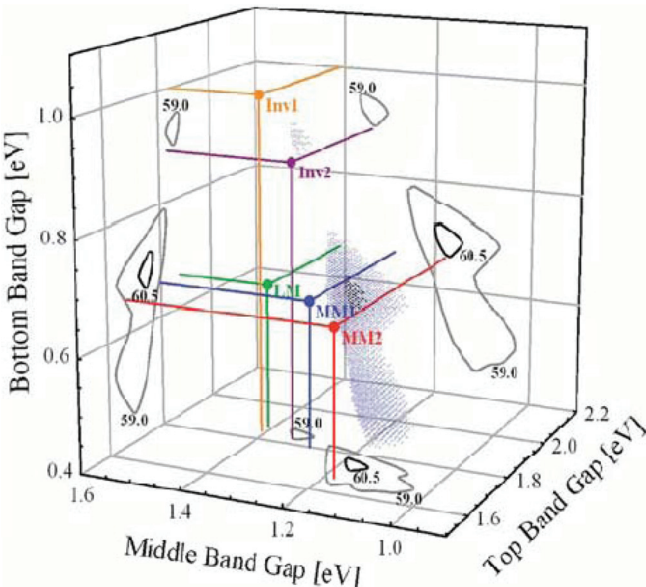


FIG. 6. (Color) Detailed balance calculations for the efficiency of different triple-junction solar cell structures under the AM1.5d ASTM G173–03 spectrum at 500 kW/m<sup>2</sup> and 298 K. The black haze represents bandgap combinations which admit efficiencies from 60.5% to 61.0% and hence mark the optimum. The gray haze represents efficiencies of 59.0–60.5% (see contours). Five specific triple junction solar cell structures are shown. The lattice-matched  $\text{Ga}_{0.5}\text{In}_{0.5}\text{P}/\text{Ga}_{0.99}\text{In}_{0.01}\text{As}/\text{Ge}$  (LM), two metamorphic GaInP/GaInAs/Ge (1.8, 1.29, 0.66 eV for MM1) and (1.67, 1.18, 0.66 eV for MM2), as well as two inverted metamorphic GaInP/GaInAs/GaInAs (1.83, 1.40, 1.00 eV for Inv1) and (1.83, 1.34, 0.89 eV for Inv2) devices. Reprinted with permission from W. Guter *et al.*, *Appl. Phys. Lett.* 94, 223504 (2009). © 2009 American Institute of Physics

removes the need of a Ge substrate. Its explanation is in Fig. 7.<sup>22</sup> First, a stack of three cells is grown on a GaAs substrate, including the bottom cell which is grown last (at the top). The upper and middle cells are grown lattice matched with the GaAs. Only the (last grown) bottom cell is metamorphic

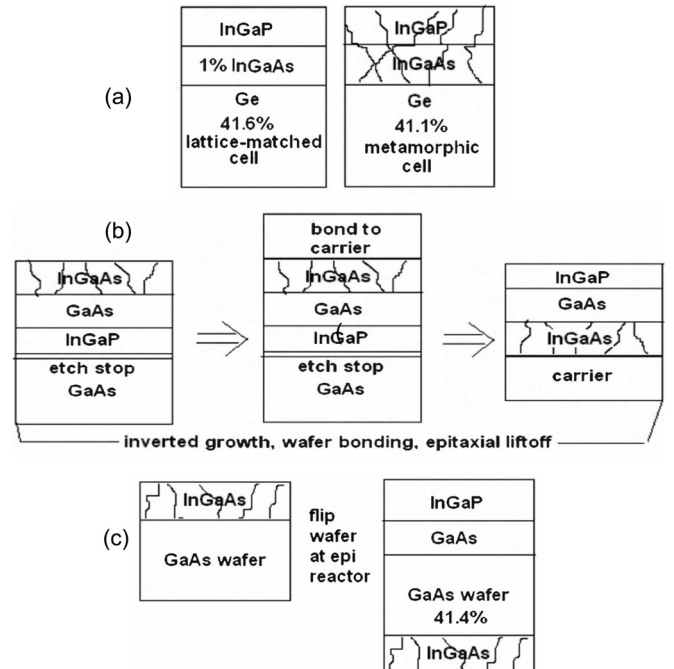


FIG. 7. (a) Lattice matched and metamorphic three-junction cell grown on Ge. Dislocations are shown in the stressed layers. (b) inverted metamorphic cell grown on GaAs, detached and bonded to carrier. (c) bifacial epitaxy metamorphic cell. Reprinted with permission from Wojciechuk *et al.*, in 35 IEEE Photovoltaic Specialists Conference, pp. 1259–1264. © 2010, IEEE.

to adjust the bandgaps. The thread dislocations are formed only in this last stage and propagate only in the bottom cell. An AlGaAs layer is first grown onto the GaAs substrate and the subsequent stack grown onto the AlGaAs layer. The AlGaAs is then etched away allowing the MJ cell to be separated from the wafer. Before etching the cell away it has to be stuck to a carrier, maybe flexible. The postprocessing steps: contacts, AR coatings, etc., are performed on this detached stack. The schematic in Fig. 7 is not complete: Tunnel junctions, buffer layers, and carrier-reflecting layers are included in appropriate stages during the growth. An efficiency of 40.8% has been obtained by NREL (USA) with an inverted metamorphic cell<sup>23</sup> of  $\text{Ga}_{0.51}\text{In}_{0.49}\text{P}/\text{Ga}_{0.96}\text{In}_{0.04}\text{As}/\text{Ga}_{0.63}\text{In}_{0.37}\text{As}$  with bandgaps<sup>23</sup> 1.83/1.34/0.89 eV. This cell is labeled in Fig. 6 as Inv2.

The bifacial epitaxy metamorphic cell concept, developed by Spire (USA), involves growing cells epitaxially on the two sides of a GaAs wafer. In the Spire process, a mismatched 0.94 eV InGaAs cell is first epitaxially grown on the back-side of a lightly doped, n-type GaAs wafer. The epi-wafer is then flipped, and 1.42 eV GaAs and 1.89 eV InGaP cells are grown lattice-matched on the opposite wafer surface. Cells are then made using only standard III-V process steps. Unlike the IMM process, the bi-facial approach does not use epitaxial lift-off and carrier bonding, but it does require that the key growth steps be performed in two separate stages and that wafer be flipped, which Spire considers to be an easy task. They have achieved the impressive record efficiency of 42.3% in the last quarter of 2010.

The use of quaternaries might give the additional degree of freedom to tune the lattice mismatch and bandgap simultaneously, but this path has yet to be explored to great extent (A GaInNAs quaternary is in the base of the 43.5% new record announced by Solar Junction while this paper was in the publication process (April 2011)). There is an initial concern relative to the low mobility of these compounds. An additional alternative has proven to be worthy of fostering: the use of nanotechnology to tune the semiconductor band gap.<sup>24,25</sup> The concept is presented in Fig. 8. Quantum Wells (QWs) are (usually) formed by growing narrow layers of a lower bandgap in a host semiconductor of higher bandgap. Due to their small size, quantum effects appear: the usual

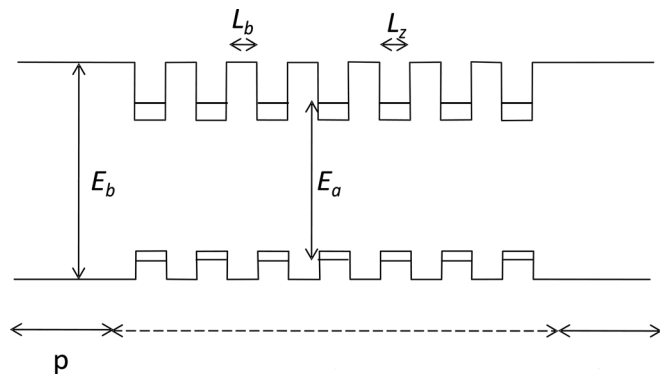


FIG. 8. Schematic band structure for a multi-QW solar cell. Reprinted with permission from K. W. J. Barnham and G. Duggan, J. Appl. Phys. 67, 3490 (1990). © 1990, American Institute of Physics.

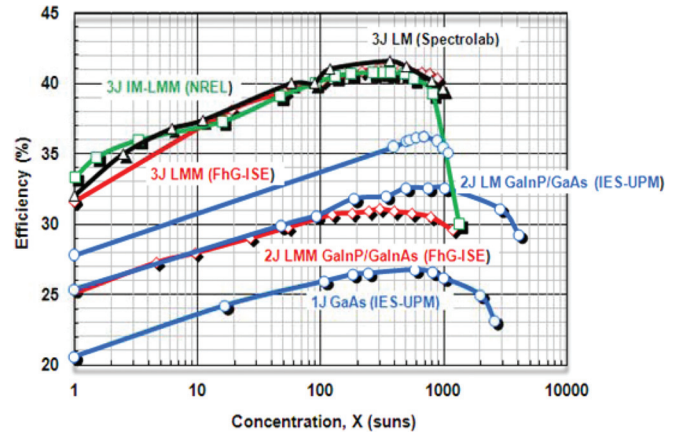


FIG. 9. (Color) Efficiency-concentration data of champion certified cells in the world.

electronic structure of the lower bandgap well material is replaced by a set of energy levels (shown in the figure) which, if the wells are close together, become continuously distributed in space, essentially modulating the conduction band edge of the composite material. In this way, the position of the top and bottom of the new bands are tuneable with the QW width; the narrower the higher the effective bandgap. Thus the bandgap may be adjusted. A problem is that the edges of the new band absorb more weakly than an ordinary band. Nevertheless, an efficiency of 28.3% at 400 suns has been achieved by Quantasol Ltd. in a QW modified GaAs solar cell which is a good result.

Fundamental study reveals that the use of concentration, implying more angularly extended illumination on the cell, leads to higher efficiency. This is also directly derived from the simple diode law in which the open circuit voltage increases logarithmically with the luminous power on the cell. As the short circuit current is roughly proportional to this power, the efficiency increases more or less logarithmically with this power flux. However, as seen in Fig. 9 (prepared by Professor Algara and coworkers at IES/UPM), at a certain concentration level the efficiency peaks and then decreases. This is because of power dissipation due to the Joule effect in different parts of the cell. The front metal grid has to be optimized to trade off Ohmic losses with grid shading factor. Ohmic losses at the grid metal-semiconductor interface are rather critical and require multiple layer solutions, both in the metal and in the semiconductor. Tunnel junctions may also be a source of efficiency loss if the tunnel junction current peak is below the current passing through the cell. In this case, a drastic voltage reduction results. In principle, higher concentration levels allow for reduction in the cell cost.

Another factor that makes concentrator cells very efficient is their high operation voltage. Many imperfections or impurities (in the space charge zone) give a dark current proportional to  $\exp(eV/2kT)$  while the fundamental radiative recombination gives a dark current proportional to  $\exp(eV/kT)$ . This means that at higher voltage the latter dominates and renders non radiative recombination, so important in solar cells at one sun, negligible.

**TABLE I.** Bandgaps and detailed balance efficiency limits for 6000/300 K Sun/ambient temperature at full concentration for unconstrained cells (not series connected). In the rightmost column, achieved efficiencies are presented or, when not available (marked with an asterisk), calculated as 70% of the detailed balance limit.

# junctions	$E_{g1}$	$E_{g2}$	$E_{g3}$	$E_{g4}$	$E_{g5}$	$E_{g6}$	Detailed B. $\eta$	%	Practical $\eta$
1	1.11						40.8 <sup>12</sup>	71.3	29.1 <sup>21</sup>
2	0.77	1.70					55.9 <sup>12</sup>	58.3	32.6 <sup>21</sup>
3	0.62	1.26	2.10				63.8 <sup>12</sup>	65.2	41.6 <sup>21</sup>
4	0.52	1.03	1.61	2.41			68.8 <sup>12</sup>	70.0	48.2*
5	0.45	0.88	1.34	1.88	2.66		72.0 <sup>27</sup>	70.0	50.4*
6	0.40	0.78	1.17	1.60	2.12	2.87	74.4 <sup>27</sup>	70.0	52.8*

The most obvious way of increasing the potential MJ cell efficiency is to add more junctions. This is not a straightforward path, but there are several prospective studies on how to proceed. The work by King *et al.*<sup>26</sup> of Spectrolab provides recommendable reading on the subject. They have, in fact, presented a four junction cell, although its efficiency is so far only 36.9%.

Will we be able to achieve 50% efficiency? What is the detailed balance potential efficiency? This is presented for the 6000/300 K sun/ambient temperatures in Table I.<sup>12,21,27</sup>

In the rightmost column, achieved efficiencies are presented. Where recorded efficiencies are unavailable (5 and 6 junctions) or represent immature technology (4 junctions), a considered practically achievable figure of 70% of the detailed balance limit is shown instead.

Observe that the 50% target is only achieved if we reach 70% of the detailed balance limit or close to it. Can we expect to achieve this 70%?

The ideal efficiencies are smaller for series connected stacks (with finite number of cells) where the additional condition of equal current in all cells is applied<sup>12,18</sup> although the difference is rather small (some tenths of an absolute percentage point of efficiency). Furthermore, the omission of the ideally selective mirrors between cells referred to above also reduces the efficiency by 1 percentage point absolute. In addition to this, the calculations in Table I. correspond to full concentration, that is to about 46 000 suns, whereas practical concentration today is in the range of 500–1000 (50–100 W cm<sup>-1</sup>) suns. In the detailed balance calculations, the efficiency increases monotonically, approximately with the logarithm of concentration, and the GaAs cell loses about two absolute points of efficiency (about 5% relative) when passing from 46 000 suns to 1000 suns. On the other hand, the terrestrial spectrum tends to produce in the same cell about two and a half absolute points of efficiency above that corresponding to the 6000 K spectrum, thus more than compensating the loss due to lower concentration. We believe that, all taken into account, if the thermodynamic limit is applied to real conditions, the values to be compared to are very similar to those in the table. However, the optimal bandgaps for real operation conditions may differ substantially from those in Table I.

A LM triple junction cell on Ge and a MM cell are presented in Ref. 28. Their efficiencies are, respectively, 40.1

and 40.7%. A detailed balance calculation for the specific bandgaps, spectrum and concentration conditions is presented (see Fig. 1 of the reference) leading to efficiencies of 50% and 53.5% for the LM and MM cases. The practical efficiencies are then 80 and 76% of the thermodynamic limit. This is indeed remarkable and leads us to believe that, with this high technological quality and the several procedures that will be used to fit the bandgaps properly without damaging the material, the achievement of 50% efficiency is very likely achievable.

It is fortunate that, in this field, because the reduction of the cell cost caused by the use of high concentration, the champion cells can, in many cases, be transferred to the market without modifications.

## B. Novel Concepts for Exceeding the SQ Limit

Adding more junctions is not an easy task. It was thought to be so and frantic attempts have started since around 2005, when the race for high efficiencies started to become established. A triple junction cell already has about 20 epi-layers and this number increase almost linearly with the number of junctions.

An elegant alternative is the use of concepts that have the potential of exceeding the SQ efficiency for each single cell. The embodied approaches are sometimes referred to as third generation concepts (although this name is also sometimes given to organic solar cells, which remain bound by the SQ limits). Three concepts are qualified as “Revolutionary Photovoltaic Devices: 50% Efficient Solar Cells” in a book edited by the USA Department of Energy.<sup>29</sup> They are the Multiple Exciton Generation (MEG) solar cell,<sup>30</sup> the Intermediate Band (IB) solar cell<sup>31</sup> and the Hot Carrier solar cell.<sup>32</sup> While the MEG is mainly developed for improving efficiency in inexpensive flat modules, the IB has a clear vocation of being used in HCPV. The hot carrier solar cell is still mainly a theoretical concept. Therefore, we shall concentrate here in the IB solar cell.

The IB solar cell consists of an IB material sandwiched between two ordinary p- and n-type<sup>31,33</sup> semiconductors (a schematic drawing is in Fig. 10).<sup>34</sup> The IB material has a band of permitted electron states within the semiconductor bandgap. Ideally this structure yields an increased current at a high voltage. The current increase comes from the fact that, in addition to the photocurrent generated by the photons with enough energy as to pump electrons from the VB to the CB, current can also be photogenerated by pairs of lower energy photons that use the IB as a stepping stone for electron-hole generation.

The current increase on its own is not that special. It can be achieved in ordinary solar cells by reducing the bandgap. The problem is that in ordinary cells the voltage is also reduced. In the IB cell the voltage is not reduced if, under illumination, the Fermi level splits into three quasi-Fermi levels, the third being for the IB.

The attractive aspect of this concept is that a single IB solar cell has a detailed balance efficiency of 62.3% compared with the 40.7% for an ordinary solar cell under full concentration for 6000/300 K sun/ambient temperature. This

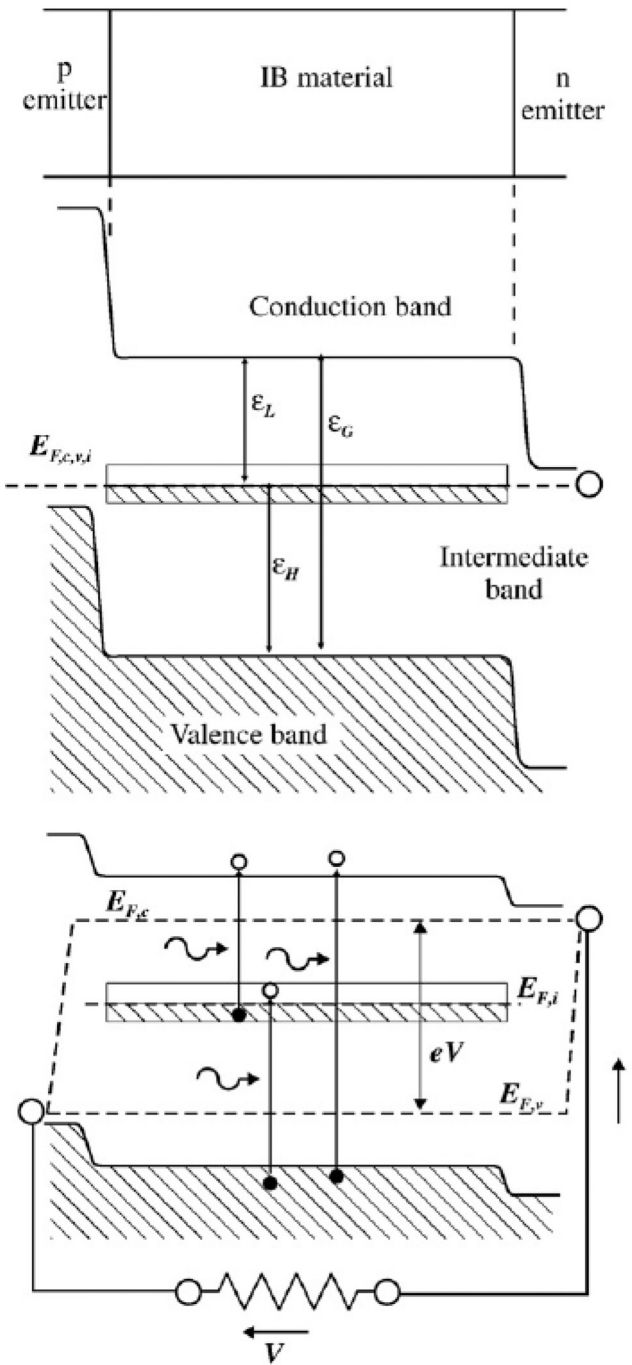


FIG. 10. (top) basic structure of an intermediate band solar cell; (middle) simplified bandgap diagram in equilibrium; (bottom) simplified bandgap diagram under illumination and forward bias. Reproduced with permission from (Canovas *et al.*, *Thin Solid Films* 516, 6943 (2008). © 2008, Elsevier.

is almost the same potential efficiency as for a triple junction solar cell (Table I).

Combinations of ordinary single junction cells (SJ) and IB cells with a tunnel junction connecting them or of two IB cell are presented in Table II.<sup>27,31,35</sup> The 70% reduction considered in Table I as the practically achievable efficiency is also calculated for the unconstrained case (not series connected). This table shows that the combination of one ordinary cell and one IB cell has a potential efficiency similar to a 4 J solar cell stack and that the combination of two IB cells is equivalent to 5 series connected solar cells. Also, in this

TABLE II. Bandgaps and the detailed balance efficiency for 6000/300 K Sun/ambient temperature at full concentration for unconstrained and series connected IB and single junction cell stacks with a single tunnel junction. In the rightmost column, 70% of the detailed balance limit is presented.

# junctions	$E_{G1}$	$E_{L1}$	$E_{G2}$	$E_{L2}$	Detail. B. $\eta$	%	Practical $\eta$
1 IB <sup>31</sup>	1.93	0.72			62.3	70.0	44.2
1 SJ up-1IB <sup>35</sup> : unconstrain.	2.39		1.59	0.55	68.6	70.0	48.0
1 SJ up-1IB <sup>35</sup> : series conn.	1.65		1.39	0.47	64.6		
1 IB up-1SJ <sup>35</sup> : unconstrain.	2.48	0.96	0.49		68.5	70.0	48.0
1 IB up-1SJ <sup>35</sup> : series conn.	2.83	1.13	0.52		67.9		
2 IB <sup>27</sup> : unconstrain.	4.00	1.73	1.25	0.44	72.6	70.0	50.8
2 IB <sup>27</sup> : series conn.	2.96	1.20	0.89	0.27	72.5		

case, with the 70% rule used for MJ cells, a practical efficiency of 50% is achievable. However, IB technology is in its infancy and forecasting its practical potential today is almost impossible.

Although the concept is very attractive, it was initially asserted that **IB materials were not possible**. However, they **can be formed by nanotechnology**: using quantum dots (QD) in a host semiconductor. The difference between a QD and a QW is that while the latter is a narrow layer of another semiconductor embedded in a host semiconductor the former are nanocrystals of the QD semiconductor surrounded entirely by the host material. Because of this 0-dimensionality, they behave as artificial atoms and present isolated levels in the host's bandgap. In contrast, the QWs present a continuous of density of states from the fundamental state to the semiconductor CB.

The isolated dots can be self assembled by depositing layers of, e.g., InAs on GaAs. These materials have a strong

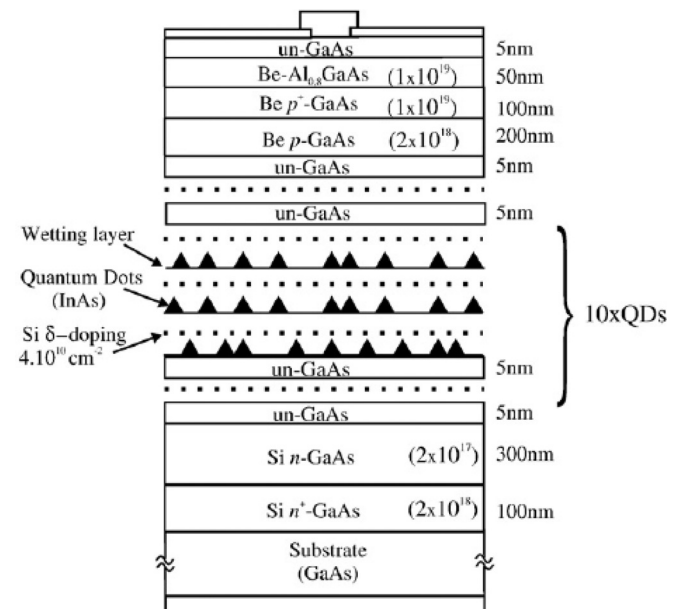


FIG. 11. Layer structure of a quantum dot intermediate band solar cell grown by molecular beam epitaxy. Reproduced with permission from (Canovas *et al.*, *Thin Solid Films* 516, 6943 (2008). © 2008, Elsevier.

lattice mismatch, as can be seen in Fig. 4. Once 2 or 3 monolayers of InAs are grown on GaAs, the InAs layer shrinks into droplets forming the QDs. In Fig. 11<sup>36,37</sup> the schematic of an IB solar cell is presented. The p region (to extract the holes) is at the top and the n region (to extract the electrons) is at the bottom. In between, the IB region is formed, in this case by 10 layers of QDs.

As observed in Table II, the bandgap of the GaAs is too far from the optimum. In fact, little improvement, if any, can be expected from this structure with respect to the ordinary GaAs cell. Indeed, the best efficiency so far is 18% at one sun,<sup>38</sup> but this structure<sup>37</sup> is well mastered and has permitted the basic principles of the IB cell operation to be proven: the two photon mechanism<sup>39</sup> and the splitting of the Fermi level into three quasi Fermi levels.<sup>40</sup>

There are several groups that have manufactured QD IB cells.<sup>37,38,41–46</sup> The main challenges associated with the manufacturing of effective IB QD cells is the increase of the absorption in the VB→IB transitions and the reduction of the size of the QDs to prevent the appearance of excited states that reduce the insulation between IB and the conduction band.<sup>47</sup> Several groups have also found bulk IB materials in certain alloys.<sup>48–53</sup> However, the cell efficiency is in the range of 1%, mainly due, we believe, to a lack of technology development for the materials used. It usually takes a long time to develop an efficient cell with a new material, even an ordinary cell. A more complete description of the topic can be found in the literature.<sup>54</sup>

#### IV. CONCENTRATOR TECHNOLOGY FOR HIGH EFFICIENCY SOLAR CELLS

The high values of efficiency presented in Fig. 1 are only possible under high luminous flux. Furthermore, they are only possible in the complex cells described in Sec. III, which can only be cost effective if producing a high electric power resulting from a high luminous power input. For this, concentrators are necessary. Although elaborate ideas are sometimes applied to designing concentrators, we are going to describe here only what we consider the canonical concentrator suitable to exploit the very high efficiency cells we have described. Such a concentrator is formed of modules that are assembled in an array containing a tracking structure. A HCPV plant is then formed of arrays arranged in subfields.

##### A. Optics for HCPV

Ultimately, the optical elements of a concentrator should be analyzed using a ray tracing program that essentially utilizes the laws of reflection and refraction. However, the manufacturing of an effective photovoltaic concentrator would hardly be possible without the support of non-imaging optics.<sup>55</sup> This discipline relies on a ray description of radiation. A ray is defined by four parameters: the position coordinates on a certain surface of the optical system—e.g., the entry aperture or the receiver surface—and the optical direction cosines (the direction cosines times the index of refraction) with respect to these coordinates. A source is defined by the optical cosines incident on each point of the entry aperture. For instance, the sun is defined at any point of the

entry aperture by a cone of rays of semiangle  $\varphi_{\text{sun}}$ . This source represents a set (bundle)  $S_e$  of rays at the entry aperture, each formed by any pair of space coordinates on the entry aperture and any angular direction within the solar cone. The problem of a concentrator may be to map this set  $S_e$  onto a set  $R$  comprising all possible rays which pass through the receiver surface. By extending the rays of the set  $S_e$ , they will reach the plane containing the receiver surface somewhere, perhaps outside the receiver itself. The goal is to have all rays reach the receiver so that  $S_e \subset R$ . The first condition to be fulfilled is that the étendue (defined in Sec. I) satisfy  $E(S_e) \leq E(R)$ . This means that the receiver cannot be as small as desired, or in other words, that the concentration is limited if rays are not to be lost. The upper limit of concentration with no ray loss is when  $S_e = R$  because in this case  $E(S_e) = E(R)$  and, since the angular extension is fixed at the entry aperture ( $\varphi_{\text{sun}}$ ), the entry aperture covers the maximum area.

A four dimensional set representing a bundle of rays, e.g.,  $S_e$ , has a boundary  $B(S_e)$  that is three dimensional. It is formed by all the rays at any point of the entry aperture which are on the surface of the cone of illumination. In the case of set  $R$ , the set  $B(R)$  is formed by all rays, regardless of direction, falling on the rim of the receiver. A very important design tool is the edge ray theorem<sup>56</sup> that states that if we map the edge rays  $B(S_e)$  onto  $B(R)$  we will assure that  $S_e \subset R$ .

If we simplify our study to a two dimensional space (e.g., for cases of rotational symmetry) the bundles of rays

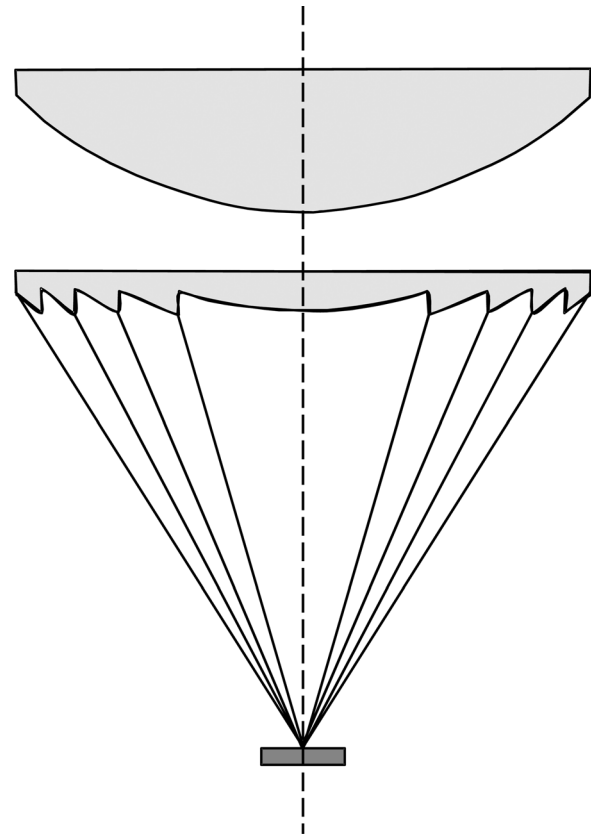


FIG. 12. Schematic of a Fresnel lens showing the teeth. Reproduced with permission from G. Sala and I. Antón, in *Handbook of Photovoltaic Science and Engineering*, 2nd edition. © 2011, Wiley.

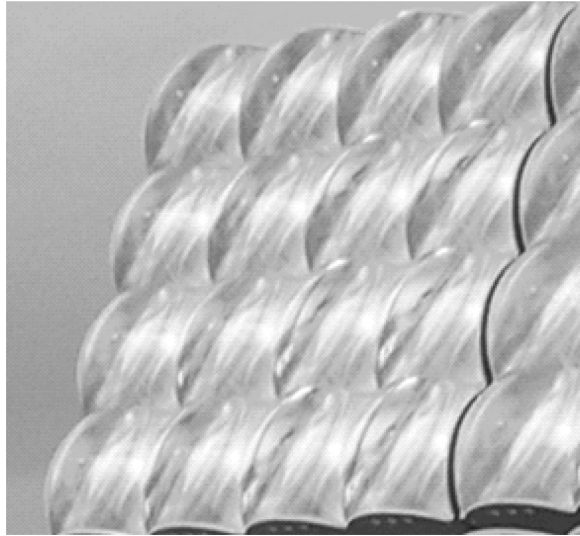


FIG. 13. Detail of the dome shaped Fresnel lenses used by Daido Steel (Japan).

have two dimensions on a surface (now represented by a line): one spatial coordinate and one angular coordinate. The edge ray theorem now requires mapping a one-dimensional bundle of rays onto another one. This can be done with, for instance, a one-dimensional mirror surface.

Leaving now the realm of the abstract, the simplest form of concentrator optics is a lens. As shown in Fig. 12,<sup>57</sup> a Fresnel lens is derived from an ordinary lens by dividing the lower surface into facets and projecting them onto the upper face in order to reduce the thickness. Most of the lenses have spherical surfaces, which are easier to manufacture, but in a Fresnel lens, made by molding or a similar technique, the angles of the facets can respond to a design different from the spherical surface giving an extra degree of freedom without extra cost. Although Fresnel lenses can be designed in a very straightforward way, the use of non-imaging optics may lead to important improvements.<sup>58</sup> For instance, as derived from this discipline,<sup>56</sup> Fresnel lenses with the shape of a dome, as shown in Fig. 13, exhibit much better characteristics.

We have discussed in Sec. II that for full collection of rays, conservation of étendue requires that the concentration decrease when the source angle increases. The problem is more acute when we consider the chromatic aberration of the lenses. Furthermore we must design our optical system so that the source angle (the acceptance angle) is higher than the sun's semiangle of about  $0.26^\circ$ . This is necessary to allow for unavoidable tracking and manufacturing errors. An acceptance angle of  $1^\circ$  might be reasonable. For this angle the maximum concentration for a Fresnel lens is in the range of 80, much less than usual in HCPV. Of course, it is possible to set a lens 1000 times larger than the solar cell but the consequence is that many rays will fall out of it and the efficiency will be reduced.

To overcome this drawback, most HCPV optics is composed of two elements, a primary optics element (POE) that is often a Fresnel lens and a secondary optics element (SOE) that can take a variety of shapes. Some are shown in Fig. 14.<sup>59</sup> The loss of rays for the case without secondary is

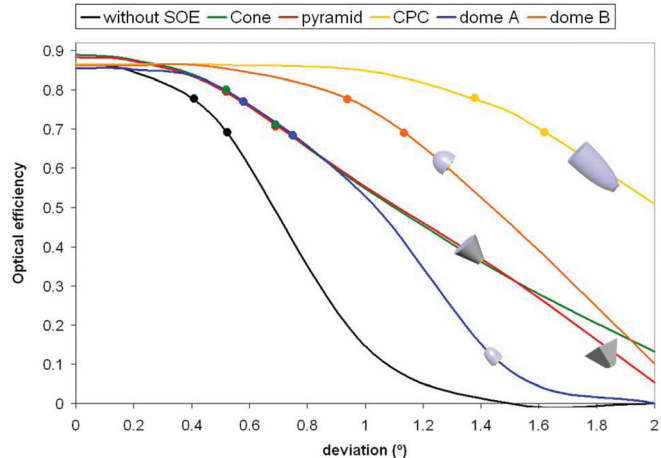


FIG. 14. (Color) Angular transmission curves for the different SOE studied. Circular marks over the lines indicate the deviation angle where optical efficiency becomes 90% and 80% of the maximum. Lens to cell geometrical concentration 1000X. Reproduced with permission from Victoria *et al.*, Opt. Express 17, 6487 (2009). © 2009, OSA.

reflected in a loss of efficiency even when the concentrator is perfectly aimed. If all the rays were collected the efficiency should be in the range of 92% corresponding to the Fresnel losses that take place when the light passes from air to an optically dense medium (about 4%) or vice versa. The pyramid and the cone are metallic and act by reflection. They only collect the spilled rays and redirect them to the cell. That is why they have the best efficiency at  $0^\circ$  deviation. The two domes and the Compound Parabolic Reflector (CPC)<sup>7</sup> are made of glass and surround the cell so increasing the étendue and permitting more acceptance angle for a given concentration, as explained in Sec. II. The CPC is the concept that permits the highest angular acceptance, but it requires more material and acts under the principle of total internal reflection, which requires its surface to be clean.

Another important requirement for concentrator optics is homogeneity of illumination. Strongly inhomogeneous illumination produces local concentrations much higher than the average leading to losses in the fill factor of the cell and reducing efficiency. A solution is the kaleidoscope, consisting of a truncated glass pyramid where the irradiance is expected to be homogenized by multiple bouncing of the rays entering it. This solution reduces substantially the acceptance angle. An interesting solution has recently been presented:<sup>60</sup> the Fresnel-Koehler (FK) concentrator that uses the principle of designing the SOE to image the POE onto the cell (see Fig. 15).<sup>60</sup> As the POE is homogeneously illuminated by the sun it produces a homogeneous light profile on it. Imaging of the POE onto the cell with the SOE can be made accurately. It produces a nice squared homogeneously illuminated area that fits with the square shape of the cell. The FK SOE has the aspect of a dome and presents an inactive optical region near the cell that favors its sticking to it. As a matter of fact in the figure the FK concentrator is formed of four independent POE-SOE couples, all the four POEs manufactured together as well as the four SOEs so that this design aspect is irrelevant for the user. Their acceptance angle is reasonably high, in the range of  $1.1^\circ$  for 1000 X.

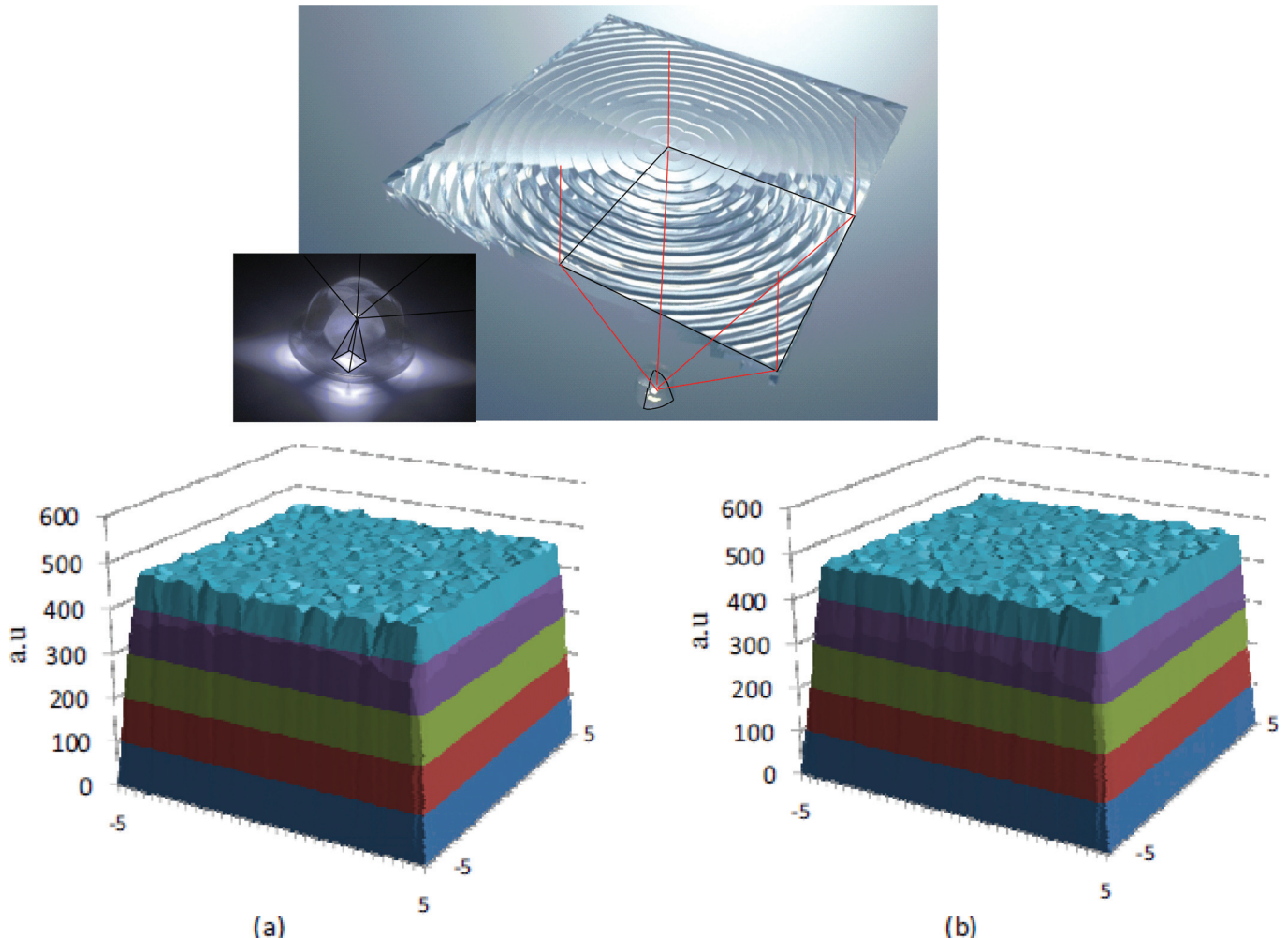


FIG. 15. (Color) Above View of the Fresnel-Koehler POE and SOE. It is formed of four POE in a single Fresnel lens each one imaged onto the cell by the four SOE elements. The four SOE elements are cast in the same block. Below: Irradiance distribution on the cell for the LPI's FK concentrator with  $C_g = 625x$ ,  $f/1$ , no AR coating on the SOE, when the sun is on axis and the solar spectrum is restricted to: (a) the top subcell range (360–690 nm), and (b) the middle-subcell range (690–900 nm). Reproduced with permission from Cveckovic *et al.*, Opt. Express 18, A25 (2010). © 2010, WIP and LPI.

It should be noticed that the optics introduces changes in the spectrum impinging the cell so that its optimum design will not be that which is used today in champion cells designed for a standard spectrum. Furthermore, due to chro-

matic aberrations, illumination profile at the cell may be different for different spectral ranges. An additional advantage of the FK concentrator is to be almost free from chromatic aberration.

Reflective optics is also used, although much less often. We present in Fig. 16<sup>57</sup> the solution of Solfocus based on non-imaging optics principles.<sup>61</sup> Its acceptance angle is rather high ( $\sim 1.4^\circ$  for 500 suns) but the efficiency is relatively low due to two metal reflections (ruled by the metal absorption) and two Fresnel reflections. Note that the element over the cell is a homogenizing kaleidoscope. Mirrors can bend rays more than lenses; therefore, this concentrator is about 3 times more compact than a refractive system for the same POE entry aperture.

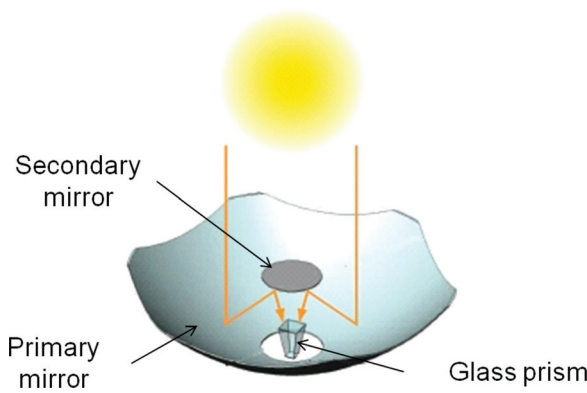


FIG. 16. (Color) The Solfocus concentrator (USA) used initially hexagonal glass reflectors in a Cassegrain structure (two mirrors) and a glass truncated pyramid coupled to multijunction cells: scheme of the principle of the concentrator. Reproduced with permission from G. Sala and I. Antón, in Handbook of Photovoltaic Science and Engineering, 2nd edition. © 2011, Wiley.

## B. HCPV Modules

Cells and optics are put in a box to form a module. The cover of the box may be a glass or more often a parquet of several Fresnel lenses that fully cover the module. In some cases, the lenses are made of transparent silicone rubber polymerized

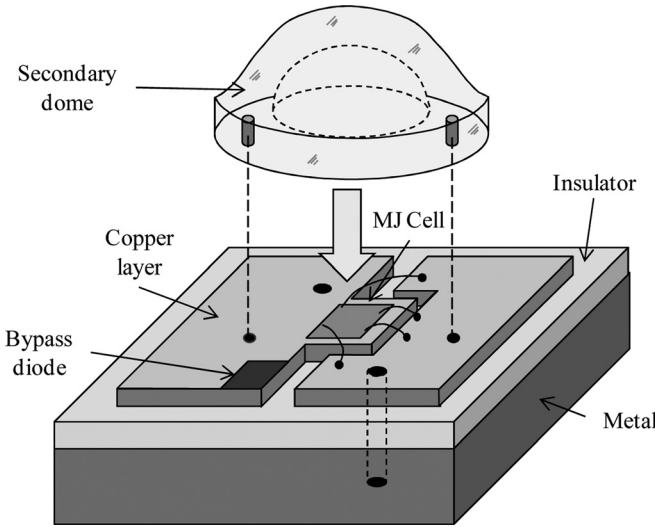


FIG. 17. Typical receiver for two-stage optics with a Fresnel lens in the primary. The substrate provides insulation and good thermal transmission. It houses a bypass diode and a dome type secondary. The hollow part of the dome is filled with silicone rubber for good optical matching. Reproduced with permission from G. Sala and I. Antón, in *Handbook of Photovoltaic Science and Engineering*, 2nd edition. © 2011, Wiley.

directly on the covering glass (hybrid lenses). In some other cases, plastic lenses are stuck onto the covering glass.

The cells have to be carefully attached to the supporting structure in such a way that the wires issuing from the solar cell be easily connected to external wires that connect to the next cell. To this end, an etched copper layer on an insulating substrate, possibly alumina, is used that must be stuck close to the metal sheet that closes the module at the back. A schematic drawing is presented in Fig. 17.<sup>57</sup> This receiver must provide easy electrical interconnection with the other cells in the module. The arrangement must provide electric insulation of all the cells, which must then be floating with respect to the module box, and thermally connected with the rear module sheet. Furthermore, a bypass diode is installed, in opposition to the cell polarity, to assure the pass of current if, for some reason, the cell finds itself in the dark. This assures that the module will operate even under partial shading and prevents the appearance of strong reverse bias in the cells, which is potentially destructive under partial shading conditions.

Several MJ cells on different substrates have been proposed for high efficient rigs with dichroic filters<sup>15</sup> that cast spectral bands of the light onto them. Efficiencies of 50% have already been planned in the USA-DARPA Program Very High Efficiency Solar Cell (VHESH) with a 5 J arrangement on three substrates<sup>62</sup> (GaInP/GaAs, Si y GaInAsP/GaInAs) and  $42.7 \pm 2.5\%$  cell (somewhat artificially) added efficiency has already been measured.<sup>63</sup> To be cost effective the several cells have to be assembled in an appropriate receiver that fulfills the requirements mentioned above.

A possible cost effective solution for four cells is under development at the LPI facilities in Madrid, Spain (an UPM spinoff).<sup>64</sup> The structure is intended for two cells and is sketched in Fig. 18. It involves a LM triple junction solar cell operating at about 500 suns and a silicon cell of about the same area operating at about 100 suns (irradiance con-

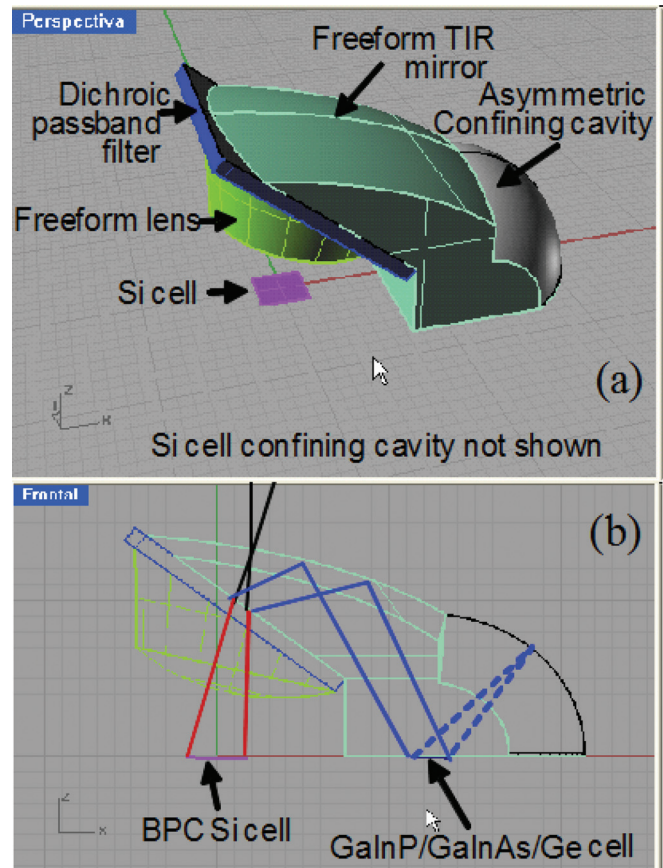


FIG. 18. (Color) The beam is split by means of a band-pass filter and directed onto two cells by means of free form optics. The filter is under medium level concentration on filter for reducing area (low cost) and good performance (moderate angular dispersion). Additionally, a mirrored cavity is recycling light reflected by the MJ cell. The optics performs the Koehler integration for good irradiance uniformity on top of cells. (a) Perspective. (b) Cross-section. (Courtesy of Prof Miñano, UPM).

centration). This cell casts onto the Si cell the part of the spectrum not absorbed by the GaInAs cell and above the Ge bandgap. In addition it uses angle limited light confining cavities<sup>65</sup> already used in a previous dichroic filter setup.<sup>15</sup> The planned added efficiency for the cells is of 47.1% for a four terminal (4 T) array and 45.2% for a 2 T array (current matched) using champion cells but the added efficient measured thus far in a 4 T simplified configuration prototype is 39.7%, with a 37.0% 3 J cell and a 25.7% silicon BPC cell.<sup>64</sup>

For single substrate structures, removing heat from the cells is not a difficult problem if the cells are small. Cooling fins are seldom used. The amount to be removed is the fraction of the power incident on the module that is not converted into electricity. This heat is partly radiated by the two faces of the module and partly removed by convection, as in the flat module case. The temperature drop in the thin insulating layer and in the metal layers is relatively small. The main concern is the removal of heat from the cell itself where the power density is high (although at 1000 suns it is still 10 times less than in high power LEDs). The typical operating temperature of the cells does not exceed 80–90 °C, that is, about 50 °C over the ambient. This is roughly twice the increase in a flat module.

Cells in modules are usually interconnected in different ways depending on the cell size, which varies between 1 mm<sup>2</sup> and 1 cm<sup>2</sup>. Usually, cells are grouped in parallel (if the cells are small) and then these groups are connected in series.

Something has to be done to keep the cells aligned given the different expansion coefficient of the glass and most metals. Also, the inside of the module must be kept clean for 25 years without dismounting it. Small tricks are used by every manufacturer that are usually kept secret.

Special equipment is being developed today for module manufacturing.<sup>66,67</sup> Collimated solar simulators for testing modules in-house (different to the simpler concentrator cell solar simulator) are already commercial and tools to measure lenses and cell/lens misalignment, etc., optically are in development. More automation will be necessary.

### C. HCPV Arrays

The tracker represents about 1/3 of the system cost so its careful consideration should not be neglected.<sup>68</sup> A typical tracker is shown in Fig. 19. A horizontal beam rotates in azimuth and in elevation on a fixed vertical axis by means of the appropriate gears and screws that are driven electrically and, in a few cases, hydraulically. A control mechanism is necessary.

The control may be based on an analog device that determines the proper orientation by the comparing shadows on several light sensors. The drawback is that although this system may aim the control device axis well, the array might be tilted with respect to this axis. Furthermore, it is sensitive to soiling. The sensor may be the output power of the array itself but this probably requires a very narrow acceptance angle that leads to losses.

Another option is to use a digital system based on calculated coordinates. In this case what we ignore are construction errors of the tracker itself (error in the South reference, departure of the vertical pedestal from the true vertical axis, tilting of the horizontal beam on the pedestal, errors on the time estimate, etc.). To determine them, a procedure has been used<sup>68,69</sup> that follows the Nobel laureate Penzias strategy to adjust big telescopes. It consists in sensing the maximum array output over the course of a sunny day (in a



FIG. 19. (Color) Inspira 36 m<sup>2</sup> tracker for HCPV modules.

relatively slow but accurate process). This gives the alignment error for many angles. An error model converts the differences into the model parameters and from that day on the corrected model is applied to follow the real sun coordinates. This method allows for fast installation because the software is very effective at correcting the installation errors.

Of great importance are the structure design and size. The construction of an array has to follow the safety codes (to withstand wind gusts, earthquakes, etc.) established in the country of utilization. This is an ultimate requirement. If the optics acceptance angle is narrow then the tracker developer has to design a very stiff structure.<sup>70</sup> However, if the optics acceptance angle is large enough the safety code assures the needed stiffness.

An additional advantage of the digital system is the potential for custom configurations such as stowing at night or under high winds, vertical orientation for inspection and other service requirements.

### D. HCPV Subfields and Fields

In 2006 a new institute—ISFOC—was created in Castilla-La Mancha, Spain, to research HCPV systems. The first action was to launch two successive international calls for tenders (the second after 1 year) that granted the installation of 3 MW of HCPV arrays. Seven companies were granted contracts: three from Spain, two from the USA, one from Germany and one from Taiwan. At present, about 2 MW are operating (some have been doing so for about 2 years) and the rest are under different states of installation and approval. One of the subfields is shown in Fig. 20. This action has permitted a wealth of unique information on the operation of HCPV at the field level.

A subfield is usually defined as the elements connected to a single inverter (clearly visible in Fig. 24), often on the order of 500 kW (although in some cases each array has its own inverter). ISFOC subfields are of 100 kW. Each company has installed between two and eight subfields.

The nominal (peak) power of flat module subfields is defined as the sum of that of the modules measured at standard test conditions (STC: 1000 W m<sup>-2</sup>, 25 °C cell temperature, spectrum defined) with a sun simulator. This concept



FIG. 20. (Color) SolFocus subfield installed at ISFOC, Puertollano, Spain.

was not applicable to the HCPV because at the time of the calls for tenders no indoor module simulator existed for concentrator modules. Furthermore, the array performance is seriously affected by the quality of the tracking control and structure.

Instead a procedure was determined to define what we called normal watt ( $W_{\text{normal}}$ ) based on measuring the arrays in the field at instances with irradiance and temperature conditions within certain limits and then applying a formula to convert the power measured into power at standard conditions. Since concentrators do not use diffuse light, the standard conditions were set as  $850 \text{ W} \cdot \text{m}^{-2}$  illumination and  $60^\circ\text{C}$  cell temperature.<sup>71</sup> These conditions are called operation test conditions (OTC).

The purpose of our definition of OTC was to facilitate a fair trade: when a customer buys a plant of say  $1 \text{ MW}_{\text{normal}}$  based on our definition, it should produce the same yearly electricity as  $1 \text{ MW}_{\text{peak}}$  of flat modules. With our definition of a normal watt, the output of a fixed plant is always much lower according to the measurements performed at ISFOC<sup>72</sup> and presented in Fig. 21. The fair comparison is, we think, with a flat panel with tracking. We can observe in this figure that our OTC are too unfavorable to HCPV (it undermines

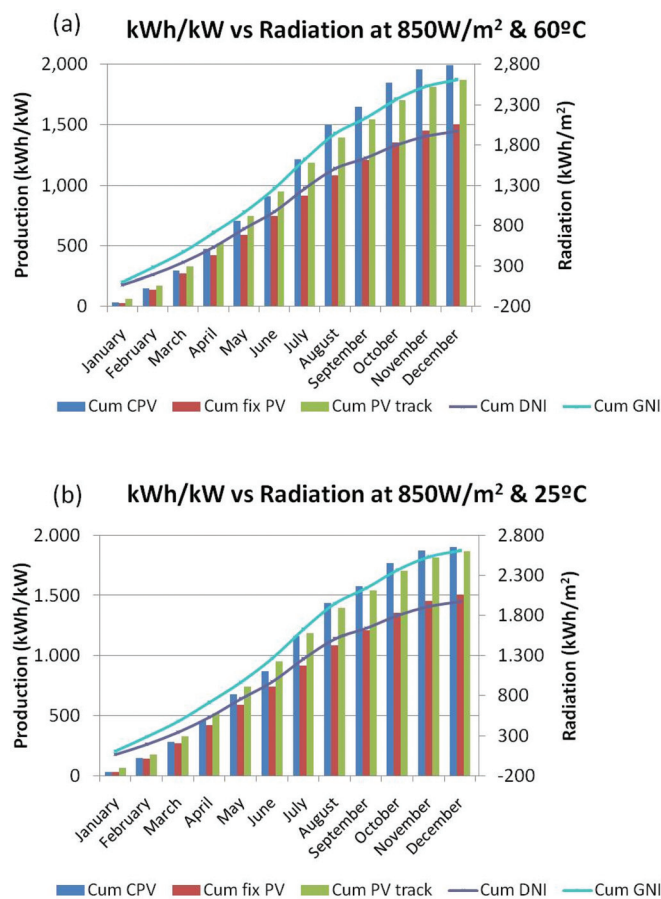


FIG. 21. (Color) Cumulated production during 2009 in a plant of ISFOC per  $\text{kW}$  ( $\text{kW}_{\text{normal}}$  in the text). The nameplate  $\text{kW}$  is measured under OTC according to the definition in the picture. This production is compared with the production per  $\text{kW}_p$  of neighboring flat module plants with and without tracking. The  $\text{kW}_p$ 's are defined under STC, as usual. Irradiation ( $\text{kWh}/\text{m}^2$ ) data are also provided (Direct normal irradiation, DNI and global normal irradiation GNI). Courtesy of F. Rubio, ISFOC.

its sale because the customer may not be aware of the higher production). A fairer comparison is produced if we use  $850 \text{ W m}^{-2}$  and  $25^\circ\text{C}$  temperature (remember that peak watts are measured at  $25^\circ\text{C}$ ).

The efficiency of an array with an individual inverter<sup>73</sup> appears in Fig. 22. It varies between 18 and 20% in the central hours of the day (due a limitation of power by the inverter to fulfill regulations, optimization might have suggested to use less modules) when most of the power is produced. It is reduced in the morning and the evening probably due to spectral mismatch. This is higher than what can be achieved with flat modules. It has to be understood that this value corresponds to technology from 2008, when the incipient commercial modules were of 20% efficiency. Today, although still incipient, they are around 30%.

What module efficiency can we expect when 50% cells become commercial? By covering the SOE with antireflection (AR) coatings, the optical efficiency is expected to exceed 90%. This would lead to module efficiency that might reach 45%. It is very likely that full plant efficiency will be around or even exceed a yearly 40%. This is to be compared to the 12% of the best plants today.

However, this efficiency is measured against the area of the modules. How does it convert into land efficiency? When installing double axis tracking arrays, either for concentrators or for flat modules, the ground cover ratio is the relevant parameter. This is the area of the modules divided by the area needed to install this array (this depends somewhat on the aspect ratio of the array, the configuration of the grid of arrays, etc.). It is presented in Fig. 23.<sup>74</sup> In this figure, the effect of partial shading of the module is to reduce the power proportionally. This is reasonable for concentration modules because of the individual bypass diodes appearing in Fig. 17. For flat modules, this is an optimistic assumption as the authors explain. A reasonable GCR is 1/5 to be compared with below 1/1.7 for fixed modules. With the definition of a normal watt for concentrators as recommended in Fig. 21, below, the  $\text{kWh}/\text{kW}$  are similar than those in Fig. 23.

What will be the ground efficiency of HCPV as compared with that of flat module PV? A guess is presented in Table III (irradiation data in Ref. 75). The ultimate HCPV efficiency follows the arguments developed above. That of

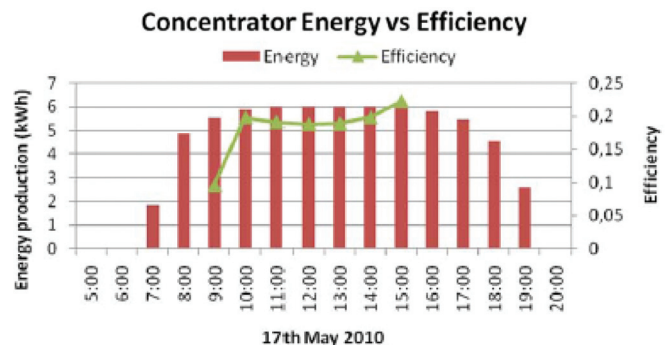


FIG. 22. (Color) AC efficiency of a 6  $\text{kW}$  array with its own inverter during a day at ISFOC, Puerto Llano, Spain. In the central hours of the day the output is limited by the inverter to avoid injecting above the permitted power. Courtesy of F. Rubio, ISFOC.

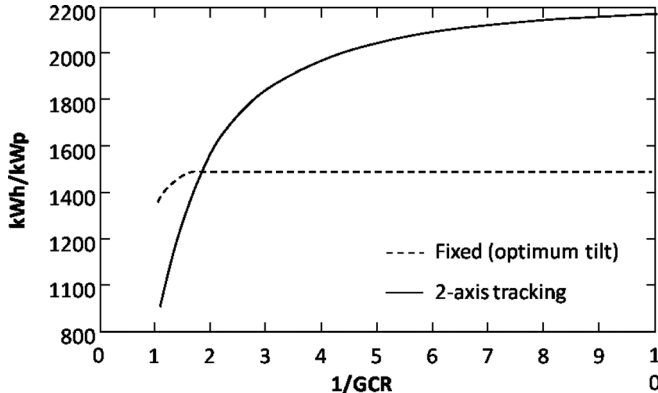


FIG. 23. Evolution of yearly energy yield in Almeria (Spain) for several tracking strategies, considering a loss of power proportional to the shading and assuming a constant soiling loss of 3%. Reprinted with permission from E. Lorenzo, in *Handbook of Photovoltaic Science and Engineering*, Chap 20. © 2003, Wiley.

the Si and organic module technology is just a guess and the plant efficiency is linked to it by the same proportion than that for HCPV. Thin film modules may be identified in efficiency with the Si technology. The conclusion of the table is that ground efficiency will be between 9 and 10% in most of the geographic areas appropriate for HCPV but will not exhibit champion efficiency. This will be reserved for fixed flat modules with ground efficiency exceeding 12%. According to our estimation, even the organic cell technology when refined will exceed the 5% ground related efficiency assumed in Sec. I of this article.

In Table IV we present data from several large scale plants that are already built. The cell efficiency is an estimation corresponding to the technology and the moment of installation. As expected, the effective GCR (calculated using the estimated efficiency) is below the 58.5% considered nec-

TABLE III. Ultimate yearly ground efficiency for two localities of good (Madrid, Spain) and excellent (Albuquerque, NM, USA) irradiation conditions and four PV technologies. Irradiation data from reference.<sup>75</sup> The irradiances on module are DNI for HCPV, GNI for Flat module tracking and global irradiance on optimally tilted modules for fixed plants.

Concept	HCPV	Si Track	Si fixed	Organic
Module efficiency	45.0%	20.0%	20.0%	10.0%
Plant efficiency	40.0%	17.8%	17.8%	8.9%
Irradiance on ground, Madrid (kWh/m <sup>2</sup> year)	1565	1565	1565	1565
Irradiance on ground, Albuquerque (kWh/m <sup>2</sup> year)	2104	2104	2104	2104
Irradiance on module, Madrid (kWh/m <sup>2</sup> year)	1878	2552	1816	1816
Irradiance on module, Albuquerque (kWh/m <sup>2</sup> year)	2904	3598	2441	2441
Electric power, Madrid (kWh/m <sup>2</sup> year)	751	454	323	161
Electric power, Albuquerque (kWh/m <sup>2</sup> year)	1162	640	434	217
GCR	20.0%	20.0%	58.8%	58.8%
Loss by self shading	6.8%	6.8%	0.0%	0.0%
Ground efficiency, Madrid	8.9%	5.4%	12.1%	6.1%
Ground efficiency, Albuquerque	10.3%	5.7%	12.1%	6.1%

TABLE IV. Specific ground coverage (MW/Ha) and estimated GCR for several large scale plants of different technologies.

Plant name	Sarnia (Canada)	Olmedilla (Spain)	Strasskirchen (Germany)	Moura (Portugal)
Plant size MW	80	60	54	46
Plant Surface (Ha)	384.5	180.0	135	250
MW/Ha	0.21	0.33	0.40	0.18
Estimated mod. $\eta$	7%	14%	14%	14%
Surface of modules (Ha)	114.3	42.9	38.6	32.9
Effective GCR	29.7%	23.8%	28.6%	13.1%

essary for in fixed modules to be shadow free. This means that considerable allowance is given to service roads and other considerations. Figure 24 shows views of some real plants presenting these allowances.

In the case of the plant at Moura (according to our efficiency estimation), the effective GCR is also well below of the 20% we consider reasonable in this paper. Even taking into account the allowances already mentioned it seems that the plant owners do not have today a big concern about the land cost.

## V. COSTS AND MARKETS

A module is the assembly of a variety of elements, most are rather conventional, a few are special (cells and optics). Different companies adopt different solutions and



FIG. 24. (Color) (top) 60 MW Olmedilla (Spain) fixed Si plant covering 180 Ha. (bottom) 46 MW Moura (Portugal) two-axes tracking flat Si module plant covering 250 Ha.

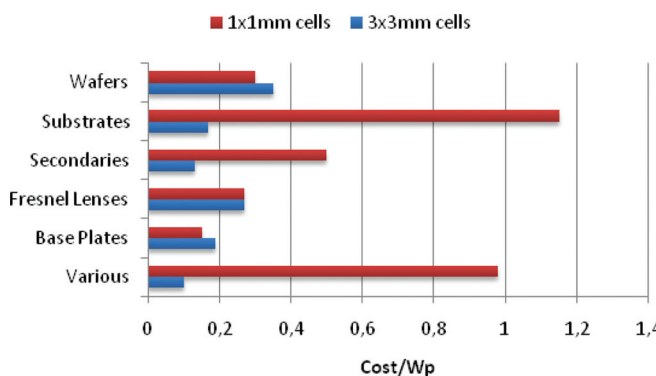


FIG. 25. (Color) Material costs for a CPV module with the following assumptions: Concentration 1000 X, module efficiency 20% 850 W/m<sup>2</sup> and 25°C. Wafers refers to the epi-wafers with the MJ cells integrated.

generalization is difficult; no attempt is made here. However, Fig. 25 presents an example describing the material costs for a specific solution (calculated by Dr. Sala of IES/UPM).

Wafer refer to the epi-wafers with the MJ cells integrated. Note that the cost of the cells (wafers) at 1000 suns is rather small. Just the elements for integrating the box, the base plates, cost almost as much. At 500 suns the cost weight of the cells is roughly double. However, the reduction of concentration may affect the costs of the substrates and other elements thus being an important element in the total cost.<sup>76,77</sup>

Most probably, today the concentrator module costs more than flat modules. But their capacity for cost reduction is much higher. This quality is often described through the so called learning curve. The production costs of most goods decrease over time following a learning curve. It is a decreasing straight line in a log-log plot with the price/cost as the ordinate and cumulated manufactured output as the abscissa. For flat modules, the price is reduced by about 21% every time the cumulated production is doubled, but for semiconductor based memory (RAM, etc.) the reduction is much higher. We have proposed<sup>78,79</sup> that this slow learning factor is associated with the fundamental efficiency limit demonstrated by the SQ model.<sup>10</sup> For HCPV, the learning curve is expected to be much faster because of two reasons: One is that many module elements and assembly techniques are not fundamental in the sense that they can be replaced by others performing a similar function, if and where this appears to be more cost effective. The second is the expected efficiency progress. Every time cell efficiency is increased the same system produces more kWh so reducing the kWh cost. The increase in efficiency may require an increase in the cell cost, but the concentration divisor makes this increase cost effective in most cases.

Concerning the tracker, if the optics is tolerant, its cost may be governed by national safety codes and therefore be similar to that of flat modules, today around 0.7 €/Wp for two axes tracking. But since the cell efficiency is expected to be about 3 times higher, the cost per W may be in the range of 0.23 €/W. This cost will be further reduced when cheaper components will be found and mass production procedures will be adopted.

The added costs associated with the subfield will be very similar to those of flat modules in fixed arrays as the increase of efficiency will balance the increased need for space.

All this taken into account, it is likely that today the cost of HCPV may be higher than that of flat modules. However, its learning curve is expected to be steeper, and therefore, its potential for reaching low costs higher. To make this potential reality, it is necessary to advance along the learning curve. Political decisions may help much in this. The 200 MW that the Italian government has reserved for concentrator plants in its scheme of feed-in tariffs is a promising approach; we shall soon see how it works. HCPV manufacturers should be aware of the need to progress and accept some loss of revenue in initiating commercialization as an investment cost with the confidence that in 2 or 3 years of manufacturing they will be ready to compete with flat modules.

## VI. STRESSES ON MATERIALS

As justified in Ref. 80, markets in the range of 100 GW per year of new installations are a reasonable goal for HCPV in the second third of this century. The first thing to realize is that HCPV, on reaching its full potential, would be to a large extent an assembly industry of volume similar to that of the car industry today. If it is profitable, this will certainly happen.

In general, no special stresses with material availability will be produced except for few mentioned here.

The development of this industry with the present triple junction cell structure will require 3.75 times the present global production of electronic grade germanium. There are some concerns on this material's availability. However, the inverted metamorphic structure does not require Ge substrates and attempts have been undertaken to form solar cells on strongly lattice mismatched Si, the second most abundant element on the Earth's crust.

The acrylic needed to make lenses will require about 1.5 times present production. The use of hybrid glass-plastic lenses would be a way of reducing acrylic utilization by 1 order of magnitude.

For the remaining materials, increased demand due to large scale HCPV should not affect global production to any great extent.

## VII. CONCLUSIONS

A sustainable civilization must obtain its energy mostly from the sun. A practically achievable step toward this would be 1/3 of electricity from the sun by the middle of this century.<sup>81</sup> The discovery of effective means of energy storage would mean this proportion could and should be increased

Efficiency is important at least to reduce costs and possibly to reduce stresses on land occupation. There are many options to extend the present cell efficiency record (above 42%) to values above 50%. Commercial cells of 50% will probably be possible.

Concentrations in the range of 1000 suns are not yet widely used, but they can reduce the cost per kW of the cells,

even if they are very sophisticated. The optics has to present an angular tolerance in the range of  $1^\circ$  (at 1000 suns) and produce homogeneous illumination even when the sun is slightly off the optical axis (but within the acceptance angle). This homogeneity must extend to all spectral ranges of the different cells in the MJ stack. Non-imaging optics is the proper tool for adequate optical design. The development of such tolerant optics at 1000 suns would free cell designers of cost constraints.

Modules must be able to accommodate cells and optics easily. Today, equipment for testing the module performance on line is becoming available and will facilitate the development of highly efficient modules at a commercial scale. Forty-five percent is probably achievable.

With tolerant optics, the trackers will not need to be bulkier than those used for flat modules. Self adjusting software will allow fast and inexpensive array mounting in the field.

The nameplate power of HCPV is a subject of discussion. In Central Spain, defining the nameplate as the power obtained with  $850 \text{ W/m}^2$  illumination and  $25^\circ\text{C}$  cell temperature would yield the same number of kWh/kW as two axes tracking installations with flat modules. This definition is probably appropriate for many more geographical zones.

Self shadowing requires that the GCR of the HCPV systems be much smaller than of flat modules. While 0.5 is reasonable for the latter, for the former it should not be much larger than 0.2. This reduces the subfield ground efficient to about 10%, somewhat below that expected for high efficiency flat module cells (12%). But the installation of HCPV on grazing land will probably be possible without hampering significantly the cattle activity.

Due to its expected fast learning curve, HCPV has the potential to become cheaper than any other PV option. To achieve this it has to compete with existing flat module technology with a learning experience of dozens of GW. HCPV will probably suffer an initial period where it will not be able to compete with flat modules unless someone is willing to support the losses of the initial steps of the learning curve. This may be public bodies or private companies. The former usually have more capacity for long term capital investment.

Some stresses on material demands will occur in the development of HCPV. Ge and acrylic for optics may cause the greatest strain. For both materials, replacements exist already today.

In summary, photovoltaics is a good choice to supply the energy we need. It has to compete for land use with food production. Where food production, with a naturally low efficiency (in the range of 0.03% from ground energy<sup>2</sup> on the arable land<sup>3</sup> to edible calories<sup>82</sup>), is expected to take up 20% of terrestrial land by mid-century (without counting pasture), we have seen here that PV ground efficiency will be in the range of 10% so that the surface needed for PV will be below 1% (and grazing will be possible in the land used for HCPV). By the middle of the century,  $1/3^{81}$  of the electricity could reasonably be produced with PV and more if inexpensive methods of energy storage are discovered. As this will be less than 20% of the total power consumed, the PV land occupation by the mid of the century will not be above 0.2%

of terrestrial lands, and this with a very strong expansion of its use.

## ACKNOWLEDGMENTS

This work has been supported by the GENESIS FV grant CSD2006-0004 of the Spanish program CONSOLIDER and by the NUMANCIA grant S-0505/ENE/0310 of the Comunidad de Madrid. The author wants to acknowledge the important text clarifications made by his co-worker Alex Mellor and by one unknown referee as well as fruitful discussion with Professors Sala and Miñano, Dr. Luque-Heredia and Ms Rubio.

- <sup>1</sup>J. R. Frisch, *Future Stresses for Energy Resources* (Graham and Trottman, London, 1986).
- <sup>2</sup>Available at [http://en.wikipedia.org/wiki/World\\_energy\\_resources\\_and\\_consumption](http://en.wikipedia.org/wiki/World_energy_resources_and_consumption). See world energy consumption data and solar energy received on ground.
- <sup>3</sup>Available at [http://en.wikipedia.org/wiki/Arable\\_land](http://en.wikipedia.org/wiki/Arable_land). See the amount of cultivated land.
- <sup>4</sup>Available at <http://www.pvresources.com/>. See the list of largest PV plants in the world, continuously updated.
- <sup>5</sup>S. Hegedus and A. Luque, in *Handbook of Photovoltaic Science and Engineering*, 2nd ed., edited by A. Luque and S. Hegedus (John Wiley and Sons, Chichester, 2011).
- <sup>6</sup>A. Luque and A. Martí, in *Handbook of Photovoltaic Science and Engineering*, 2nd ed., edited by A. Luque and S. Hegedus (John Wiley and Sons, Chichester, 2011).
- <sup>7</sup>R. Winston, *Sol. Energy* **16**, 89 (1974).
- <sup>8</sup>P. T. Landsberg and G. Tonge, *J. Appl. Phys.* **51**, R1 (1980).
- <sup>9</sup>R. Winston and W. T. Welford, *Optics of Non Imaging Concentrators* (Academic, New York, 1979).
- <sup>10</sup>W. Shockley and H. J. Queisser, *J. Appl. Phys.* **32**, 510 (1961).
- <sup>11</sup>J. L. Balenzategui and A. Martí, *Sol. Energy Mater. Sol. Cells* **90**, 1068 (2006).
- <sup>12</sup>G. L. Araujo and A. Martí, *Sol. Energy Mater. Sol. Cells* **33**, 213 (1994).
- <sup>13</sup>R. Hulstrom, R. Bird, and C. Riordan, *Sol. Cells* **15**, 365 (1985).
- <sup>14</sup>A. Martí and G. L. Araújo, *Sol. Energy Mater. Sol. Cells* **43**, 203 (1996).
- <sup>15</sup>A. Martí, P. A. Davies, J. Olivan, C. Algora, M. J. Terron, J. Alonso, J. C. Maroto, G. L. Araujo, J. C. Minano, G. Sala, and A. Luque, in *Conference Record of the Twenty Third IEEE Photovoltaic Specialists Conference - 1993* (IEEE, New York, 1993), p. 768–773.
- <sup>16</sup>X. T. Wang, N. Waite, P. Murcia, K. Emery, M. Steiner, F. Kiamilev, K. Goossen, C. Honsberg, and A. Barnett, in *2009 34th IEEE Photovoltaic Specialists Conference, Vols 1–3* (IEEE, New York, 2009), pp. 223–228.
- <sup>17</sup>D. J. Friedman, J. M. Olson, and S. Kurtz, in *Handbook of Photovoltaic Science and Engineering*, 2nd ed., edited by A. Luque and S. Hegedus (John Wiley and Sons, Chichester, 2011).
- <sup>18</sup>I. Tobías and A. Luque, *Prog. Photovoltaics: Res. Appl.* **10**, 323 (2002).
- <sup>19</sup>W. Guter, J. Schone, S. P. Philipps, M. Steiner, G. Siefer, A. Wekkeli, E. Welser, E. Oliva, A. W. Bett, and F. Dimroth, *Appl. Phys. Lett.* **94**, 223504 (2009).
- <sup>20</sup>M. A. Green, K. Emery, D. L. King, Y. Hisikawa, and W. Warta, *Prog. Photovoltaics Res. Appl.* **14**, 45 (2006).
- <sup>21</sup>M. A. Green, K. Emery, Y. Hisikawa, and W. Warta, *Prog. Photovoltaics* **18**, 346 (2010).
- <sup>22</sup>S. Wojtczuk, P. Chiu, X. Zhang, D. Derkacs, C. Harris, D. Pulver, and M. Timmons, in *35 IEEE Photovoltaic Specialists Conference* (IEEE, Honolulu, 2010), pp. 1259–1264.
- <sup>23</sup>J. F. Geisz, D. J. Friedman, J. S. Ward, A. Duda, W. J. Olavarria, T. E. Moriarty, J. T. Kiehl, M. J. Romero, A. G. Norman, and K. M. Jones, *Appl. Phys. Lett.* **93**, 3 (2008).
- <sup>24</sup>K. W. J. Barnham and G. Duggan, *J. Appl. Phys.* **67**, 3490 (1990).
- <sup>25</sup>N. J. Ekins-Daukes, K. W. J. Barnham, J. P. Connolly, J. S. Roberts, J. C. Clark, G. Hill, and M. Mazzer, *Appl. Phys. Lett.* **75**, 4195 (1999).
- <sup>26</sup>R. R. King, A. Boca, W. Hong, X.-Q. Liu, D. Bhusari, D. Larabee, K. M. Edmondson, D. C. Law, C. M. Fetzer, S. Mesropian, and N. H. Karam, in *24th European Photovoltaic Solar Energy Conference* (Hamburg, Germany, 2009), p. 55–61.

- <sup>27</sup>E. Antolín, A. Martí, and A. Luque, in *Proc. of the 21st European Photovoltaic Solar Energy Conference*, edited by J. Poortmans, H. Ossenbrink, E. Dunlop, and P. Helm (WIP-Renewable Energies, Munich, 2006), pp. 412–415.
- <sup>28</sup>R. R. King, D. C. Law, K. M. Edmondson, C. M. Fetzer, G. S. Kinsey, H. Yoon, R. A. Sherif, and N. H. Karam, *Appl. Phys. Lett.* **90**, 183516 (2007).
- <sup>29</sup>N. S. Lewis, G. Crabtree, A. J. Nozik, M. R. Wasielewski, and P. Alivisatos, *Basic Research Needs for Solar Energy Utilization*, US DOE ([http://www.sc.doe.gov/bes/reports/files/SEU\\_rpt.pdf](http://www.sc.doe.gov/bes/reports/files/SEU_rpt.pdf)) (2005).
- <sup>30</sup>S. Kolodinski, J. H. Werner, T. Witchen, and H. J. Queisser, *Appl. Phys. Lett.* **63**, 2405 (1993).
- <sup>31</sup>A. Luque and A. Martí, *Phys. Rev. Lett.* **78**, 5014 (1997).
- <sup>32</sup>R. T. Ross and A. J. Nozik, *J. Appl. Phys.* **53**, 3813 (1982).
- <sup>33</sup>A. Luque and A. Martí, *Prog. Photovoltaics* **9**, 73 (2001).
- <sup>34</sup>E. Cánovas, A. Martí, N. López, E. Antolín, P. G. Linares, C. D. Farmer, C. R. Stanley, and A. Luque, *Thin Solid Films* **516**, 6943 (2008).
- <sup>35</sup>E. Antolín, “Development of Experimental Techniques for the Demonstration of the Operation Principles of the Intermediate Band Solar Cell,” Doctoral Thesis, UPM, Madrid, 2010.
- <sup>36</sup>E. Canovas, A. Martí, D. Fuertes-Marrón, E. Antolín, G.-L. P., and A. Luque, in *Proc. 23th European Photovoltaic Conference* (WIP, Valencia, 2008), pp. 298–303.
- <sup>37</sup>A. Luque, A. Martí, C. Stanley, N. López, L. Cuadra, D. Zhou, and A. McKee, *J. Appl. Phys.* **96**, 903 (2004).
- <sup>38</sup>S. A. Blokhin, A. V. Sakharov, A. M. Nadtochy, A. S. Pauysov, M. V. Maximov, N. N. Ledentsov, A. R. Kovsh, S. S. Mikhrin, V. M. Lantratov, S. A. Mintairov, N. A. Kaluzhniy, and M. Z. Shvarts, *Semiconductors* **43**, 514 (2009).
- <sup>39</sup>A. Martí, E. Antolín, C. R. Stanley, C. D. Farmer, N. Lopez, P. Diaz, E. Canovas, P. G. Linares, and A. Luque, *Phys. Rev. Lett.* **97**, 247701 (2006).
- <sup>40</sup>A. Luque, A. Martí, N. Lopez, E. Antolín, E. Canovas, C. Stanley, C. Farmer, L. J. Caballero, L. Cuadra, and J. L. Balenzategui, *Appl. Phys. Lett.* **87**, 083505 (2005).
- <sup>41</sup>S. M. Hubbard, C. D. Cress, C. G. Bailey, R. P. Raffaelle, S. G. Bailey, and D. M. Wilt, *Appl. Phys. Lett.* **92**, 123512 (2008).
- <sup>42</sup>R. Oshima, A. Takata, and Y. Okada, *Appl. Phys. Lett.* **93**, 083111 (2008).
- <sup>43</sup>V. Popescu, G. Bester, M. C. Hanna, A. G. Norman, and A. Zunger, *Phys. Rev. B* **78**, 205321 (2008).
- <sup>44</sup>D. Zhou, G. Sharma, S. F. Thomassen, T. W. Reenaas, and B. O. Fimland, *Appl. Phys. Lett.* **96**, 061913 (2010).
- <sup>45</sup>D. Alonso-Alvarez, A. G. Taboada, J. M. Ripalda, B. Alen, Y. Gonzalez, L. Gonzalez, J. M. Garcia, F. Briones, A. Martí, A. Luque, A. M. Sanchez, and S. I. Molina, *Appl. Phys. Lett.* **93**, 123114 (2008).
- <sup>46</sup>J. Phillips, K. Kamath, X. Zhou, N. Chervela, and P. Bhattacharya, *J. Vac. Sci. Technol. B* **16**, 1243–1346 (1997).
- <sup>47</sup>P. G. Linares, A. Martí, E. Antolín, and A. Luque, *J. Appl. Phys.* **109**, 014313 (2011).
- <sup>48</sup>K. M. Yu, W. Walukiewicz, J. Wu, W. Shan, J. W. Beeman, M. A. Scarfulla, O. D. Dubon, and P. Becla, *Phys. Rev. Lett.* **91**, 246403 (2003).
- <sup>49</sup>K. M. Yu, W. Walukiewicz, J. W. Ager, III, D. Bour, R. Farshchi, O. D. Dubon, S. X. Li, I. D. Sharp, and E. E. Haller, *Appl. Phys. Lett.* **88**, 092110 (2006).
- <sup>50</sup>N. Lopez, L. A. Reichertz, K. M. Yu, K. Campman, and W. Walukiewicz, *Phys. Rev. Lett.* **106**, 028701 (2011).
- <sup>51</sup>R. Lucena, I. Aguilera, P. Palacios, P. Wahnon, and J. C. Conesa, *Chem. Mater.* **20**, 5125 (2008).
- <sup>52</sup>G. Gonzalez-Diaz, J. Olea, I. Martí, D. Pastor, A. Martí, E. Antolín, and A. Luque, *Sol. Energy Mater. Sol. Cells* **93**, 1668 (2009).
- <sup>53</sup>W. Wang, A. S. Lin, and J. D. Phillips, *Appl. Phys. Lett.* **95**, 011103 (2009).
- <sup>54</sup>A. Luque and A. Martí, *Adv. Mater.* **22**, 160 (2009).
- <sup>55</sup>R. Winston, J. C. Miñano, and P. Benítez, *Non Imaging Optics* (Elsevier, Burlington, 2005).
- <sup>56</sup>A. Luque, *Solar Cells and Optics for Photovoltaic Concentration* (Adam Hilger, Bristol, 1989).
- <sup>57</sup>G. Sala and I. Antón, in *Handbook of Photovoltaic Science and Engineering*, 2nd ed., edited by A. Luque and S. Hegedus (John Wiley and Sons, Chichester, 2011).
- <sup>58</sup>R. Leutz and A. Suzuki, *Nonimaging Fresnel Lenses: Design and Performance of Solar Concentrators* (Springer, Berlin, 2001).
- <sup>59</sup>M. Victoria, C. Dominguez, I. Anton, and G. Sala, *Opt. Express* **17**, 6487 (2009).
- <sup>60</sup>P. Benítez, J. C. Minano, P. Zamora, R. Mohedano, A. Cvetkovic, M. Buljan, J. Chaves, and M. Hernandez, *Opt. Express* **18**, A25 (2010).
- <sup>61</sup>R. Winston and J. R. M. Gordon, *Opt. Letters* **30**, 2617 (2005).
- <sup>62</sup>A. Barnett, D. Kirkpatrick, C. B. Honsberg, D. Moore, M. Wanlass, K. Emery, R. Schwartz, D. Carlson, S. Bowden, D. Aiken, A. Gray, S. Kurtz, L. Kazmerski, T. Moriarty, M. Steiner, J. Gray, T. Davenport, R. Buelow, L. Takacs, N. Shatz, J. Bortz, O. Jani, K. Goossen, F. Kiamilev, A. Doolittle, I. Ferguson, B. Unger, G. Schmidt, E. Christensen, and D. Salzman, in *Milestones Toward 50% Efficient Solar Cell Modules*, Milano, 2007 (WIP), pp. 95–100.
- <sup>63</sup>A. Barnett, D. Kirkpatrick, C. Honsberg, D. Moore, M. Wanlass, K. Emery, R. Schwartz, D. Carlson, S. Bowden, D. Aiken, A. Gray, S. Kurtz, L. Kazmerski, M. Steiner, J. Gray, T. Davenport, R. Buelow, L. Takacs, N. Shatz, J. Bortz, O. Jani, K. Goossen, F. Kiamilev, A. Doolittle, I. Ferguson, B. Unger, G. Schmidt, E. Christensen, and D. Salzman, *Prog. Photovoltaics* **17**, 75 (2009).
- <sup>64</sup>P. Benítez, R. Mohedano, M. Buljan, J. C. Minano, Y. Sun, W. Falicoff, J. Vilaplana, J. Chaves, G. Biot, and J. Lopez, in *7th International Conference on Concentrating Photovoltaic Systems, CPV-7* (Las Vegas, 2011) PSE, Freiburg, in the press.
- <sup>65</sup>J. C. Minano, A. Luque, and I. Tobias, *Applied Optics* **31**, 3114–3122 (1992).
- <sup>66</sup>C. Dominguez, I. Anton, G. Sala, and Ieee, in *Pvsc: 2008 33rd Ieee Photovoltaic Specialists Conference, Vols 1–4* (Ieee, New York, 2008), p. 1575–1579.
- <sup>67</sup>C. Dominguez, S. Askins, I. Anton, G. Sala, and Ieee, in *2009 34th Ieee Photovoltaic Specialists Conference, Vols 1–3* (Ieee, New York, 2009), p. 123–127.
- <sup>68</sup>I. Luque-Heredia, Autocalibrated Sun Tracking Control Systems. From theory & implementation to volume production (Dr. Thesis, UPM, Madrid, 2010).
- <sup>69</sup>I. Luque-Heredia, C. Martin, M. T. Mananes, J. M. Moreno, J. L. Auger, V. Bodin, J. Alonso, V. Diaz, and G. Sala, in *Proceedings of 3rd World Conference on*; Vol. 1 (2003), pp. 857–860.
- <sup>70</sup>I. Luque-Heredia, G. Quémére, P. H. Magalhães, L. Hermanns, A. F. d. Lerma, and A. Luque, in *Proceedings of the 21st European Photovoltaic Solar Energy Conference* (WIP, IMunich, 2006), pp. 2105–2109.
- <sup>71</sup>F. Rubio, M. Martinez, J. Perea, D. Sanchez, and P. Banda, in *2009 34th IEEE Photovoltaic Specialists Conference, Vols. 1–3* (IEEE, New York, 2009), pp. 707–712.
- <sup>72</sup>F. Rubio, M. Martínez, A. Martín, A. Hipólito, and P. Banda, in *6th International Conference on Concentrating Photovoltaic Systems* (American Institute of Physics, lFreiburg, 2010), pp. 252–255.
- <sup>73</sup>F. Rubio, M. Martínez, A. Hipólito, A. Martín, and P. Banda, in *25th EU Photovoltaics Solar Energy Conference* (WIP, lValencia, 2010), pp. 1008–1011.
- <sup>74</sup>L. Narvarte and E. Lorenzo, *Prog. Photovoltaics* **16**, 703 (2008).
- <sup>75</sup>E. Lorenzo, in *Handbook of Photovoltaic Science and Engineering*, edited by A. Luque and S. Hegedus (John Wiley and Sons, Chichester, 2003), Chap 20.
- <sup>76</sup>M. Yamaguchi and A. Luque, *IEEE Trans. Electron Dev.* **46**, 2139 (1999).
- <sup>77</sup>C. Algara, in *Next Generation Photovoltaics: High Efficiency Through Full Spectrum Utilization*, edited by A. Martí and A. Luque (Institute of Physics, Bristol, 2004).
- <sup>78</sup>A. Luque, *Prog. Photovoltaics* **9**, 303 (2001).
- <sup>79</sup>A. Luque and A. Martí, in *Next Generation Photovoltaics: High Efficiency through Full Spectrum Utilization*, edited by A. Martí and A. Luque (Institute of Physics Publishing, Bristol, 2003), pp. 1–18.
- <sup>80</sup>G. Sala and A. Luque, in *Concentrator Photovoltaics*, edited by A. Luque and V. M. Andreev (Springer, Berlin, 2007), pp. 1–24.
- <sup>81</sup>T. B. Johansson, H. Kelly, A. K. N. Reddy, R. H. Williams, and L. Burnham, *Renewable Energy Sources for Fuel and Electricity* (Island Press, Washington, DC, 1993).
- <sup>82</sup>Available at <http://www.fao.org/fileadmin/templates/ess/img/chartroom/151.jpg>, edited by FAO. See the average world consumption of calories.